

Freeze-in Production of Sterile Neutrino Dark Matter in $U(1)_{B-L}$ Model

Anirban Biswas¹, Aritra Gupta²

Harish-Chandra Research Institute, Chhatnag Road, Jhansi, Allahabad 211 019, INDIA

ABSTRACT

With the advent of new and more sensitive direct detection experiments, scope for a thermal WIMP explanation of dark matter (DM) has become extremely constricted. The non-observation of thermal WIMP in these experiments has put a strong upper bound on WIMP-nucleon scattering cross section and within a few years it is likely to overlap with the coherent neutrino-nucleon cross section. Hence in all probability, DM may have some non-thermal origin. In this work we explore in detail this possibility of a non-thermal sterile neutrino DM within the framework of $U(1)_{B-L}$ model. The $U(1)_{B-L}$ model on the other hand is a well-motivated and minimal way of extending the standard model so that it can explain the neutrino masses via Type-I see-saw mechanism. We have shown, besides explaining the neutrino mass, it can also accommodate a non-thermal sterile neutrino DM with correct relic density. In contrast with the existing literature, we have found that W^\pm decay can also be a dominant production mode of the sterile neutrino DM. To obtain the comoving number density of dark matter, we have solved here a coupled set of Boltzmann equations considering all possible decay as well as annihilation production modes of the sterile neutrino dark matter. The framework developed here though has been done for a $U(1)_{B-L}$ model, can be applied quite generally for any models with an extra neutral gauge boson and a fermionic non-thermal dark matter.

¹Email: anirbanbiswas@hri.res.in

²Email: aritra@hri.res.in

1 Introduction

The existence of Dark Matter (DM) in the Universe is now an acceptable reality. There are various satellite borne experiments, namely WMAP [1] and Planck [2] who have already measured the current mass density (relic density) of DM in the Universe with an extremely good accuracy. Moreover, there are also some indirect evidences about the existence of dark matter such as flatness of galactic rotation curve [3], gravitational lensing of distant object [4], bullet cluster [5] etc. However the composition of DM is still unknown to us. The Standard Model (SM) of electroweak interaction does not have any fundamental particle which can play the role of DM. Hence in order to accommodate a viable dark matter candidate we need to formulate a theory beyond Standard Model (BSM) of electroweak interaction. Among the various possible BSM theories available in literature the Weakly Interacting Massive Particle (WIMP) is the most favourable class of dark matter candidates and until now neutralino in the Supersymmetric Standard Model is one of the most studied WIMPs [6]. The presence of DM is also being investigated in various direct detection experiments, namely LUX [7], XENON 100 [8] etc, and no “real signal” due to a dark matter particle has been observed yet. With the increasing sensitivity of the direct detection experiments (“ton-scale”) [9, 10, 11], the WIMP-nucleon cross section is soon to merge with the elastic neutrino-nucleon cross section [12, 13]. The floor mostly comprises of 8_{B} and 7_{Be} solar neutrinos [14]. Hence in future our only probe to distinguish a dark matter signal (assuming that DM is a thermal WIMP) from the neutrino background will be through directional searches [15]. But if we wish to move beyond this thermal WIMP scenario, there is another class of dark matter candidates which are produced through non-thermal processes at an early stage of the Universe. Such possibilities include axino [16, 17, 18], gravitino [19, 20], very heavy dark matter candidates like WIMPzillas [21] among many others [22]. Their interaction strengths with other particles (in the thermal plasma) are so feeble that they never attain thermal equilibrium. These types of dark matter candidates are known as Feebly Interacting Massive Particle or FIMP [23]. In contrast with the commonly discussed WIMP scenario, the relic density of FIMP type dark matter is attained by the so called Freeze-in mechanism [23]. Unlike the thermal Freeze-out mechanism where relic density depends on the final abundance of dark matter, in Freeze-in, DM relic density is sensitive to its initial production history (for a nice review see [24]). In literature two types of Freeze-in mechanisms are usually discussed, IR (infra-red) Freeze-in [25, 26, 27] and UV (ultra-violet) Freeze-in [28, 29, 30]. Unlike the former, the DM relic density in UV Freeze-in depends explicitly on the reheat temperature (T_{R}). Production of the non-thermal DM candidate usually occurs via a decay of a heavy mother particle (e.g. from Inflaton decay and decay of heavy Moduli fields [31, 32]).

In this work we will study a FIMP type dark matter candidate in the $U(1)_{\text{B-L}}$ extension

of the Standard Model of particle physics. $U(1)_{B-L}$ extension of SM is a very well motivated BSM theory as it provides the explanation of nonzero neutrino mass through Type-I sea-saw mechanism. In this model besides the usual SM gauge $(SU(3)_c \times SU(2)_L \times U(1)_Y)$ symmetry, an additional local $U(1)_{B-L}$ symmetry invariance is also imposed on the Lagrangian where B and L respectively represent the baryon and lepton number of a particle. In order to obtain an “anomaly free gauge theory”, three additional right handed neutrinos ($N_i, i = 1, 3$) are required to be added to the particle spectrum of SM. Moreover, we also require a complex scalar (Ψ) which is a singlet under the SM gauge group but possesses a suitable nonzero $U(1)_{B-L}$ charge. Majorana masses for the three right handed neutrinos are generated through the spontaneous breaking of the local $B - L$ symmetry by the vacuum expectation value (VEV) of complex scalar singlet Ψ . The lightest one (N_1) among the three right handed neutrinos can be a viable dark matter candidate.

The dark matter candidate N_1 in $U(1)_{B-L}$ model can be produced through both thermal as well as non-thermal processes. In the former case, the interaction strengths of DM particles with others in the early Universe are such that they are able to maintain their thermal as well as chemical equilibrium. The decoupling of the DM particles occur when their interaction rates fall short of the expansion rate of the Universe. If n_{eq} and $\langle\sigma v\rangle$ are the equilibrium number density and the thermally averaged annihilation cross section of N_1 then the decoupling condition requires $\frac{n_{eq}\langle\sigma v\rangle}{H} < 1$ with H being the Hubble parameter. Being out of equilibrium, the relic density of N_1 freezes to a particular value which depends upon the interaction strength as well as the temperature of the Universe at which the decoupling occurred (freeze-out temperature). The thermally produced N_1 as a dark matter candidate, in the $U(1)_{B-L}$ extension of SM, has been studied in Refs.[33, 34, 35, 36]. In these works most of the authors have shown that the relic abundance of dark matter particle satisfied the WMAP or Planck limit only when the mass of DM is nearly half the masses of mediating scalar particles (at or near resonances). This requires significant fine tuning as there is no symmetry, in the Lagrangian, which can relate the masses of dark matter and the scalar sector particles in the above mentioned way. Hence, with respect to the above discussions, it is natural to think about a dark matter particle, in this $U(1)_{B-L}$ model, which is produced through some non-thermal interactions at the early stage of the Universe. Non-thermal sterile neutrino production from the oscillation of active neutrinos was first proposed by Dodelson-Widrow [37], but this idea is now in conflict with the X-ray observations [38]. Other mechanisms of sterile neutrino production like Shi-Fuller mechanism [39] can alleviate some of these problems producing a colder dark matter spectrum. Several other models have also successfully discussed non-thermal sterile neutrino dark matter. They include some Supersymmetric models [40], models using warped extra-dimensions [41] and decay from charged [42] and neutral scalars [43, 44] or from extra gauge bosons [45, 46]. Most of the

studies involving production of sterile neutrino from extra gauge boson assume the gauge boson to be in thermal equilibrium with the other SM particles. However, in this work we have moved away from this assumption (details later). Several non-thermal models of sterile neutrino dark matter under the assumption of low reheating temperature have also been studied in [47, 48, 49] which is also not the case we are considering here.

Additionally, unlike what is usually done in building a dark matter model, we do not impose any extra symmetry to stabilise our dark matter candidate. For an \mathcal{O} (MeV) sterile neutrino dark matter we have a dominant decay mode to e^\pm and ν with a very large life time (larger than the age of the Universe for the parameters we consider here) which in turn helps us to propose a possible indirect detection signal of the 511 keV line observed by INTEGRAL/SPI [50] of ESA.

The rest of the paper is organised as follows: In Section 2 we briefly describe the $U(1)_{B-L}$ model. In Section 3 we describe the production mechanism of non-thermal sterile neutrino dark matter in detail. Section 4 describes the Boltzmann equation(s) needed to compute the comoving number densities of both Z_{BL} and N_1 . Calculation of relic density of sterile neutrino dark matter is given in Section 5. Section 6 deals with a possible indirect detection mode of our dark matter particle N_1 . Finally our conclusion is given in Section 7. All analytic expressions of decay widths and annihilation cross sections used in this work are listed in the Appendix.

2 The $U(1)_{B-L}$ extension of Standard Model

In the present work we have considered a *minimal* $U(1)_{B-L}$ extension of the Standard Model where the SM gauge sector is enhanced by an additional local $U(1)_{B-L}$ gauge symmetry with B and L are known as the baryon and lepton number of a particle. Therefore, under the $U(1)_{B-L}$ gauge group all SM leptons (including neutrinos) and quarks have charges -1 and $\frac{1}{3}$ respectively. Besides the SM fields, this model requires the presence of three right handed neutrinos (N_i , $i = 1$, to 3) with $U(1)_{B-L}$ charge -1 for anomaly cancellation. On the other hand, as the SM Higgs doublet (Φ) does not possess any $B - L$ charge, hence in order to spontaneously break the local $B - L$ symmetry one needs to introduce a scalar field which transforms nontrivially under the $U(1)_{B-L}$ symmetry group. As a result, the scalar sector of the present model is composed of a usual Higgs doublet (doublet under $SU(2)_L$) Φ and a complex scalar singlet Ψ . To generate Majorana mass terms in a gauge invariant manner for the three right handed neutrinos one needs the $B - L$ charge of Ψ is $+2$. $B - L$ symmetry is spontaneously broken when Ψ acquires VEV v_{BL} while the remnant electroweak symmetry ($SU(2)_L \times U(1)_Y$) of the Lagrangian breaks spontaneously through the usual Higgs mechanism. In unitary gauge, the expressions of Φ and

Ψ , after getting VEVs v and v_{BL} respectively, are

$$\Phi = \begin{pmatrix} 0 \\ \frac{\phi+v}{\sqrt{2}} \end{pmatrix}, \quad \Psi = \frac{\psi + v_{\text{BL}}}{\sqrt{2}}. \quad (1)$$

The gauge invariant and renormalisable Lagrangian of the scalar sector is thus given by

$$\mathcal{L}_{\text{scalar}} = (D_{\phi\mu}\Phi)^\dagger(D_\phi^\mu\Phi) + (D_{\psi\mu}\Psi)^\dagger(D_\psi^\mu\Psi) - V(\Phi, \Psi), \quad (2)$$

with

$$\begin{aligned} V(\Phi, \Psi) = & \mu_1^2(\Phi^\dagger\Phi) + \lambda_1(\Phi^\dagger\Phi)^2 + \mu_2^2(\Psi^\dagger\Psi) + \lambda_2(\Psi^\dagger\Psi)^2 \\ & + \lambda_3(\Phi^\dagger\Phi)(\Psi^\dagger\Psi), \end{aligned} \quad (3)$$

where

$$\begin{aligned} D_{\phi\mu}\Phi &= \left(\partial_\mu + i\frac{g}{2}\sigma^a W_{a\mu} + i\frac{g'}{2}B_\mu \right) \Phi, \\ D_{\psi\mu}\Psi &= (\partial_\mu + iQ_{\text{BL}}(\Psi)g_{\text{BL}}Z_{\text{BL}\mu})\Psi, \end{aligned} \quad (4)$$

are the covariant derivatives of the scalar doublet Φ and complex scalar singlet Ψ respectively while $Q_{\text{BL}}(\Psi) = +2$ is the B – L charge of Ψ . Gauge couplings of $\text{SU}(2)_\text{L}$, $\text{U}(1)_\text{Y}$ and $\text{U}(1)_{\text{B-L}}$ are denoted by g , g' and g_{BL} . The corresponding gauge fields are $W_{a\mu}$ ($a = 1, 2, 3$), B_μ and $Z_{\text{BL}\mu}$. After spontaneous breaking of $\text{SU}(2)_\text{L} \times \text{U}(1)_\text{Y} \times \text{U}(1)_{\text{B-L}}$ symmetry by the VEVs of Φ and Ψ we get two physical neutral scalar fields h and H which can be expressed as a linear combinations of ϕ and ψ in the following way

$$\begin{pmatrix} h \\ H \end{pmatrix} = \begin{pmatrix} \cos\theta & -\sin\theta \\ \sin\theta & \cos\theta \end{pmatrix} \begin{pmatrix} \phi \\ \psi \end{pmatrix}, \quad (5)$$

where θ is the mixing angle between the neutral scalars h and H . The expressions of mixing angle (θ) and masses (M_h , M_H) of h and H are given by

$$\begin{aligned} \theta &= \frac{1}{2} \tan^{-1} \left(\frac{\lambda_3 v_{\text{BL}} v}{\lambda_2 v_{\text{BL}}^2 - \lambda_1 v^2} \right), \\ M_h^2 &= \lambda_1 v^2 + \lambda_2 v_{\text{BL}}^2 - \sqrt{(\lambda_1 v^2 - \lambda_2 v_{\text{BL}}^2)^2 + (\lambda_3 v v_{\text{BL}})^2}, \\ M_H^2 &= \lambda_1 v^2 + \lambda_2 v_{\text{BL}}^2 + \sqrt{(\lambda_1 v^2 - \lambda_2 v_{\text{BL}}^2)^2 + (\lambda_3 v v_{\text{BL}})^2}. \end{aligned} \quad (6)$$

We have considered the physical scalar h as the SM-like Higgs boson which was discovered recently by ATLAS [51] and CMS [52] collaborations and consequently we have fixed the value

of M_h at 125.5 GeV. Also according to the measured values of Higgs boson signal strengths (for its various decay modes) the mixing angle θ between the SM-like Higgs boson h and extra scalar boson H should be very small. As this mixing angle does not play any significant role in the present context, we have kept θ fixed at 0.1 rad [53], throughout this work, such that it satisfies all results from both ATLAS and CMS collaborations. Besides this, in order to obtain a stable vacuum the quartic couplings of the Lagrangian (Eq. 3) must satisfy the following inequalities,

$$\begin{aligned}\lambda_1 &\geq 0, \\ \lambda_2 &\geq 0, \\ \lambda_3 &\geq -2\sqrt{\lambda_1\lambda_2}.\end{aligned}\tag{7}$$

Moreover, as both Φ and Ψ have nonzero VEVs, this requires $\mu_i^2 < 0$ ($i = 1, 2$).

The gauge sector Lagrangian of the present model is given as ¹

$$\mathcal{L}_{\text{gauge}} = \mathcal{L}_{\text{gauge}}^{\text{SM}} - \frac{1}{4}Z'_{\mu\nu}Z'^{\mu\nu}.\tag{8}$$

Here, $\mathcal{L}_{\text{gauge}}^{\text{SM}}$ is the Lagrangian of the SM gauge sector while the second term represents the kinetic term for the B – L gauge bosons Z_{BL} and in terms of Z_{BL} the field strength tensor $Z'^{\mu\nu}$ for an abelian gauge field is defined as

$$Z'^{\mu\nu} = \partial^\mu Z_{\text{BL}}^\nu - \partial^\nu Z_{\text{BL}}^\mu.\tag{9}$$

The gauge invariant Lagrangian for the three right handed neutrinos can be written as:

$$\mathcal{L}_{\text{RN}} = i \sum_{i=1}^3 \bar{N}_i \not{D}_N N_i - \lambda_{R_i} \bar{N}_i^c N_i \Psi + \sum_{\alpha=1}^3 \sum_{i=1}^3 y_{\alpha i} \bar{L}_\alpha \tilde{\Phi} N_i,\tag{10}$$

where $\tilde{\Phi} = -i\tau_2\Phi^*$ and $\not{D}_N = \gamma_\mu D_N^\mu$ with

$$D_N^\mu N_i = (\partial_\mu - i g_{\text{BL}} Z_{\text{BL}\mu}) N_i\tag{11}$$

is the covariant derivative for the right handed neutrino N_i . After $U(1)_{\text{B-L}}$ symmetry breaking the masses of right handed neutrinos and Z_{BL} are given by

$$M_{Z_{\text{BL}}}^2 = 4g_{\text{BL}}^2 v_{\text{BL}}^2,\tag{12}$$

$$M_{N_i} = \sqrt{2}\lambda_{R_i} v_{\text{BL}}.\tag{13}$$

¹In general we may also have a kinetic mixing term given by $\kappa Z_{\mu\nu}Z'^{\mu\nu}$. The value of κ is however severely constrained by electroweak precision measurements ($\kappa \lesssim 10^{-4}$ [54]). So for calculational simplicity we have restricted ourselves to a parameter space where $\kappa < g_{\text{BL}}$, hence neglecting its contribution. These type of scenarios where kinetic mixing term is neglected has been previously studied under the name of “Minimal/Pure” $U(1)_{\text{B-L}}$ model [33, 34, 55].

Using above two equations one can write the coupling λ_{R_i} in terms of g_{BL} , M_{N_i} and $M_{Z_{\text{BL}}}$ which is

$$\lambda_{R_i} = \sqrt{2} \left(\frac{M_{N_i}}{M_{Z_{\text{BL}}}} \right) g_{\text{BL}}. \quad (14)$$

From Eq. (10) it is possible to generate neutrino masses via Type-I see-saw mechanism. In our analysis we want to focus on the viability of lightest sterile neutrino (N_1) as a dark matter candidate. So for simplicity we have neglected intergenerational mixing between the active and sterile neutrinos. The mass of the other two sterile neutrinos are also not constrained by our analysis in this work, and in principle can be very heavy aiding neutrino mass generation by the see-saw mechanism. From Eq. (10) and Eq. (13), one can find the expression of active-sterile mixing angle α_i per generation as

$$\tan 2\alpha_i = -\frac{\sqrt{2}y_i v}{M_{N_i}}. \quad (15)$$

For simplicity, throughout this work we have denoted the first generation active-sterile mixing angle α_1 by only α .

The non-observation of the extra neutral gauge boson in the LEP experiment [56, 57] imposes following constraint ² on the ratio of $M_{Z_{\text{BL}}}$ and g_{BL} :

$$\frac{M_{Z_{\text{BL}}}}{g_{\text{BL}}} = 2v_{\text{BL}} \geq 6 - 7 \text{ TeV}. \quad (16)$$

In our analysis independent parameters are:

Mass of the extra singlet Higgs M_H , Masses of all three RH neutrinos M_{N_i} , mass of extra neutral gauge boson $M_{Z_{\text{BL}}}$, scalar mixing angle θ , the new gauge coupling g_{BL} and active-sterile mixing angle α . In terms of our chosen independent set of model parameters, the other parameters appearing in Eq. (3) can be written as

$$\mu_1^2 = -\frac{v(M_h^2 + M_H^2) + (M_h^2 - M_H^2)(v \cos 2\theta - v_{\text{BL}} \sin 2\theta)}{4v}, \quad (17)$$

$$\mu_2^2 = \frac{-v^3(M_h^2 + M_H^2) + (M_h^2 - M_H^2)(v^3 \cos 2\theta + v_{\text{BL}}^3 \sin 2\theta)}{4v v_{\text{BL}}^2}, \quad (18)$$

$$\lambda_1 = \frac{M_h^2 + \cos 2\theta(M_h^2 - M_H^2) + M_H^2}{4v^2}, \quad (19)$$

$$\lambda_2 = \frac{\cos 2\theta(M_H^2 - M_h^2) + M_h^2 + M_H^2}{4v_{\text{BL}}^2}, \quad (20)$$

$$\lambda_3 = \frac{\sin \theta \cos \theta (M_H^2 - M_h^2)}{v v_{\text{BL}}}. \quad (21)$$

²For recent bounds on $M_{Z_{\text{BL}}}$ and g_{BL} from the LHC experiment see Ref. [58].

3 Exploring the Non-thermal Regime

Non-thermal production mechanism of dark matter has been studied for quite a long time. Their characteristic behaviour comes from the very low cross section with the Standard Model particles in the early Universe. Due to this very low cross section (lower than that of WIMPs), the non-thermal dark matter particles can never reach in thermal equilibrium with the Standard Model particles. Hence their evolution in the early Universe is studied differently than the thermal scenario. In the thermal scenario, the abundance of a relic particle (called WIMP) remains nonzero in the present epoch due to the “Freeze-out” mechanism [59], whereas in the case of a non-thermal production of DM (called FIMP), a different mechanism known as “Freeze-in” [23] is responsible for their relic abundance. In the non-thermal case, due to very low interaction cross section, the initial abundance of the dark matter is taken to be zero. As the Universe cools, they are dominantly produced by the decay of other SM/BSM particles. They can also be produced by the scattering of SM/BSM particles, but with a sub-dominant contribution. Once the non-thermal dark matter is produced, due to extremely low interaction strength, they do not thermalise with the rest of the thermal soup. Since most of the production of DM particles in the non-thermal regime occur from the decays of heavier particles, non-thermality condition will be satisfied when the rate of production from the decaying mother particle (decay width) is less than the expansion rate of the Universe at around a temperature $T \sim M$, where M is the mass of the decaying particle [60]. Mathematically this can be written as

$$\frac{\Gamma}{H} < 1 \quad (\text{for } T \sim M), \quad (22)$$

where, Γ is the relevant decay width and H is the Hubble parameter. However in some cases, if the production of DM particles may occur mainly from the annihilation of other particles in the thermal bath (production from decay can be forbidden due to kinematical condition or by some symmetry in the Lagrangian). Γ will then be replaced by:

$$\Gamma = n_{eq} \langle \sigma v \rangle, \quad (23)$$

where, $\langle \sigma v \rangle$ is the thermally averaged annihilation cross section of the particles in the thermal bath and n_{eq} is their *equilibrium* number density.

In this $U(1)_{B-L}$ model, to calculate the relic density of a non-thermal sterile neutrino dark matter (N_1), the principal ingredient is its production from various decay and annihilation channels. This gives the required comoving number density of N_1 upon solving the relevant Boltzmann equation. The main production channels of the sterile neutrino (via decay) are :

$$W^\pm \rightarrow N_1 e^\pm, Z \rightarrow N_1 \bar{N}_1, Z_{BL} \rightarrow N_1 \bar{N}_1, H \rightarrow N_1 \bar{N}_1, h \rightarrow N_1 \bar{N}_1.$$

The corresponding decay widths are given in the Appendix A.1. As discussed earlier, non-thermal

dark matter particles can also be produced from the scattering of the SM/BSM particles in the thermal soup. The rate of the back reactions are negligible, since the number density of N_1 is extremely small in the early Universe. The annihilation channels along with corresponding cross sections aiding the production of N_1 are also given in the Appendix A.2. As we will see later, in the present case W^\pm and Z_{BL} decays are main production channels of N_1 . Using the non-thermality condition given in Eq. (22) we find that the extra gauge coupling g_{BL} and the active-sterile mixing angle α must be less than 10^{-9} and 10^{-7} (rad) respectively for an $\mathcal{O}(\text{MeV})$ sterile neutrino with the mass of Z_{BL} lying in 1 GeV to 100 GeV range. Although this is a simple way to estimate the order of magnitude of g_{BL} and α required for the dark matter candidate (N_1) to be non-thermal, this sets a very first upper limit on these quantities. However, more stringent upper bound on α ($\alpha \lesssim 10^{-9}$ rad) arises from the stability of DM over the cosmological time scale.

Moreover, an upper bound on the active-sterile mixing angle α is also obtained from the invisible decay of the Standard Model Z boson. Following Ref. [61] we find:

$$\frac{\Gamma(Z \rightarrow \text{inv})}{\Gamma(Z \rightarrow \nu\nu)} = 2.990 \pm 0.007. \quad (24)$$

In the limit when active-sterile mixing angle is small and $M_Z \gg M_{N_1}$, from the above equation we get $\sin^4 \alpha < 0.007$. As we will see later that for us, this condition is indeed being satisfied. In the present scenario since $M_h < 2 M_H$, SM Higgs boson can decay *invisibly* only into a pair of lightest sterile neutrino N_1 . From the expression of the decay width given in Eq. (37) we find that it is suppressed by g_{BL}^2 and hence very small. Thus this decay width easily satisfies the bound on invisible decay of SM Higgs boson from LHC [62]. Furthermore, due to sufficiently small interaction strength with the SM particles, non-thermally produced N_1 always satisfies all the existing bounds on spin independent as well as spin dependent scattering cross sections from dark matter direct detection experiments [7].

We have mentioned earlier that for the non-thermal production of the sterile neutrinos, the coupling constant g_{BL} should be very small ($< 10^{-9}$). As is usually done, while considering the production of dark matter from a decay of any SM/BSM particle, the latter is implicitly assumed to be in thermal equilibrium. Hence we usually do not need to solve a system of *coupled* Boltzmann equations, since the equilibrium number density is assumed for the decaying mother particle. But, here due to very low interaction strength of Z_{BL} (due to small g_{BL}), it will not be in thermal equilibrium with the rest of the particles. Also, the decay of Z_{BL} is a mode of production of the our sterile neutrino dark matter N_1 . So, first, we find the comoving number density of Z_{BL} by solving its Boltzmann equation. Then we use this to find the relic density of our sterile neutrino dark matter. Thus, in our case we have to solve a set of two *coupled* Boltzmann equations, one for the sterile neutrino dark matter, and another for the Z_{BL} .

In any model with a sterile neutrino we will have an active-sterile mixing in general. Hence in such model *production* of the sterile neutrino via W^\pm decay is a very generic feature. But, it is usually not taken into account since it is suppressed by the square of the small active-sterile mixing angle. However, in this work, in our favoured parameter space, we find that a sizeable contribution (to the relic-density of N_1) even from the W^\pm decay is present (see Section 4.1). Another important feature which will be present for a generic model having a nonzero active sterile mixing is the production of sterile neutrino through the Dodelson-Widrow (DW) mechanism. Here the production of sterile neutrino occurs via the oscillations of active neutrinos to the sterile ones. But this mechanism suffers serious drawbacks from the Lyman- α bounds [63] as well as X-ray observations [38]. It is now known [64, 65] that sterile neutrino produced by this mechanism cannot comprise the whole of the dark matter of the Universe. The contribution arising to the relic abundance of a sterile neutrino from the DW mechanism is given by [66]

$$\Omega_{\text{DW}} h^2 \approx 0.3 \times \left(\frac{\sin^2 2\alpha}{10^{-10}} \right) \left(\frac{M_{N_1}}{100 \text{ keV}} \right)^2, \quad (25)$$

where, α is the active sterile mixing angle and M_{N_1} is the mass of the sterile neutrino. In our case we find (see Section 5 for details) that in order to satisfy relic density, α should be less than 10^{-10} rad for sterile neutrino mass lying between 1 MeV and 10 MeV. From Eq. (25) we see that the corresponding DW contribution to the relic density is $\lesssim 1.2 \times 10^{-6}$ and hence negligible.

4 Boltzmann Equation

In this section, we write the two coupled Boltzmann equations that dictates the final relic abundance of the sterile neutrino dark matter N_1 . The Boltzmann equation for the evolution of Z_{BL} which, as already discussed is very weakly interacting is given by ³:

$$\frac{dY_{Z_{\text{BL}}}}{dz} = \frac{2M_{pl}}{1.66 M_h^2} \frac{z \sqrt{g_\star(z)}}{g_s(z)} \left(\langle \Gamma_{H \rightarrow Z_{\text{BL}} Z_{\text{BL}}} \rangle Y_H^{eq} - \langle \Gamma_{Z_{\text{BL}} \rightarrow all} \rangle Y_{Z_{\text{BL}}} \right). \quad (26)$$

Here, $Y_{Z_{\text{BL}}} \equiv \frac{n_{Z_{\text{BL}}}}{s}$ is the comoving number density of the extra gauge boson with $n_{Z_{\text{BL}}}$ and s being the number density of Z_{BL} and the entropy density of the Universe respectively. Also $z \equiv \frac{\Lambda}{T}$ where Λ is a mass scale and T is the temperature of the Universe. For simplicity we have

³In general the first term of Eq. (26) will look like: $\langle \Gamma_{H \rightarrow Z_{\text{BL}} Z_{\text{BL}}} \rangle (Y_H^{eq} - Y_{Z_{\text{BL}}})$, but since the initial abundance of Z_{BL} is very small, we have neglected the inverse process i.e. $Z_{\text{BL}} Z_{\text{BL}} \rightarrow H$, and consequently dropping the $\langle \Gamma_{H \rightarrow Z_{\text{BL}} Z_{\text{BL}}} \rangle Y_{Z_{\text{BL}}}$ term in our analysis.

taken $\Lambda \sim M_h$, the mass of SM Higgs boson while M_{pl} is the usual Planck mass. The function $g_\star(z)$ is given by:

$$\sqrt{g_\star(z)} = \frac{g_s(z)}{\sqrt{g_\rho(z)}} \left(1 - \frac{1}{3} \frac{d \ln g_s(z)}{d \ln z} \right),$$

where, $g_\rho(z)$ and $g_s(z)$ are the effective degrees of freedom related to the energy density ρ and the entropy density s of the Universe respectively. The quantity $\langle \Gamma_{A \rightarrow BB} \rangle$ denotes the thermally averaged decay width for the process $A \rightarrow BB$ and its expression, in terms of decay width $\Gamma_{A \rightarrow BB}$, is given by [67]⁴:

$$\langle \Gamma_{A \rightarrow BB} \rangle = \frac{K_1(z)}{K_2(z)} \Gamma_{A \rightarrow BB}. \quad (27)$$

Here, $K_1(z)$ and $K_2(z)$ are the modified Bessel functions of order 1 and 2 respectively. The expressions for the relevant decay widths are given in Appendix A.3.

The SM particles acquire their masses after the process of EWSB whereas the BSM particles like $U(1)_{B-L}$ gauge boson Z_{BL} and the additional Higgs boson (H) gain their masses after the breaking of $U(1)_{B-L}$ symmetry. Therefore, in the early Universe the main production channel of the new gauge boson is mainly through the decay of H , while the latter is in thermal equilibrium with the plasma. The first term in Eq. (26) denotes this contribution to the production of Z_{BL} (i.e. increase in number density of Z_{BL}) and hence comes with a positive sign. Since in our case, both the masses of Z_{BL} and H are free parameters, we have adopted the values of M_H in a range such that it always satisfy the kinematical condition $M_H \geq 2 M_{Z_{BL}}$. Although in the early stage of the Universe, the decay of H is the main production channel of Z_{BL} , in principle it can also be produced from the annihilation processes, involving both SM as well as BSM particles, like $hh \rightarrow Z_{BL} Z_{BL}$, $W^+ W^- \rightarrow Z_{BL} Z_{BL}$, $ZZ \rightarrow Z_{BL} Z_{BL}$, $HH \rightarrow Z_{BL} Z_{BL}$, $N_{2,3} \bar{N}_{2,3} \rightarrow Z_{BL} Z_{BL}$ etc. However, contribution of these annihilation processes is subleading to that of decay. The number density of extra gauge boson Z_{BL} is also depleted mainly through its decay modes to $N_1 \bar{N}_1$ (other two sterile neutrinos are assumed to be heavy for simplicity), $\nu_x \bar{\nu}_x$ and $f \bar{f}$. It is denoted by the second term in the Boltzmann equation (Eq. (26)), and as expected it comes with a negative sign, since it signifies the depletion of Z_{BL} number density. These two competing processes (production vs. depletion) decide the final comoving number density of Z_{BL} . Numerically solving Eq. (26), we graphically show the evolution of comoving number density of Z_{BL}

⁴For a more rigorous approach, when the decaying particle is Z_{BL} , one should use its non-thermal distribution function ($f_{Z_{BL}}$) for calculating this thermally averaged decay width. The expression will look like: $\langle \Gamma_{Z_{BL} \rightarrow BB} \rangle = \frac{\int (\frac{M_{Z_{BL}}}{E_{Z_{BL}}}) \Gamma_{Z_{BL} \rightarrow BB} f_{Z_{BL}}(p, T) d^3 p}{\int f_{Z_{BL}}(p, T) d^3 p}$. The non-thermal distribution function $f_{Z_{BL}}$ should be obtained first by solving the appropriate Boltzmann equation.

with $z = \frac{M_h}{T}$ in Fig. 1.

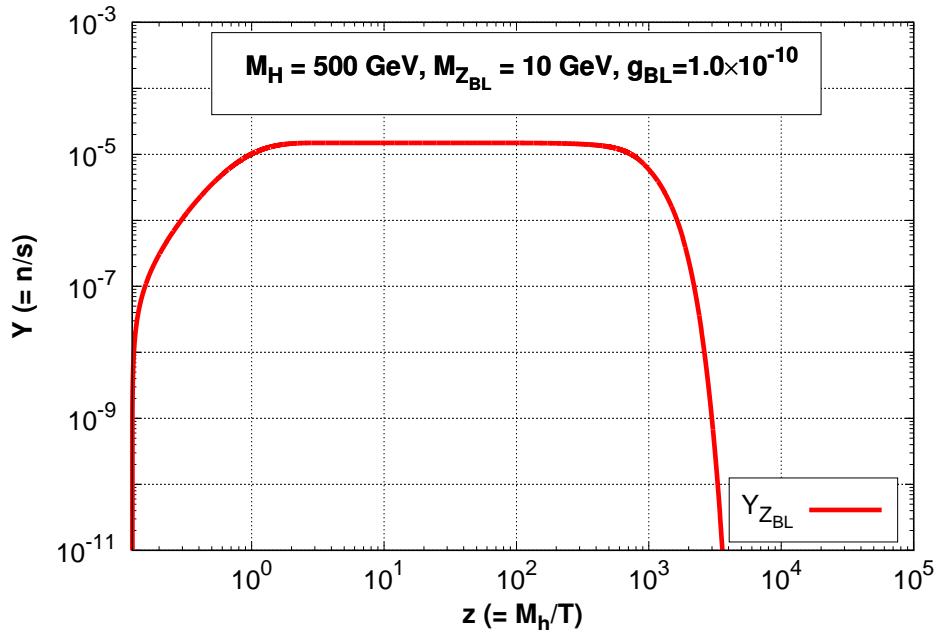


Figure 1: Evolution of comoving number density of Z_{BL} with respect to z .

From the above plot it is seen that, the comoving number density of Z_{BL} first rises due to the production term (first term in the R.H.S. of Eq. (26)) and then after a certain time it falls when the depletion term (i.e. the second term in the R.H.S. of Eq. (26)) begins to dominate. This situation arises because, at that time the temperature of the Universe becomes much smaller than M_H ($T \ll M_H$) and hence, being a non relativistic species, the equilibrium number density of H is exponentially suppressed. Therefore, the production of Z_{BL} ceases. The middle “plateau” like portion occurs when both the production and the depletion terms are comparable and hence compensating each other. The plot is generated for the following chosen set of relevant parameters: $M_H = 500$ GeV, $M_{Z_{BL}} = 10$ GeV and $g_{BL} = 10^{-10}$.

Now, we proceed to write the Boltzmann equation of the lightest sterile neutrino N_1 . This will govern the number density of the dark matter candidate (N_1) and consequently its relic abundance at the present epoch. Similar to Eq. (26), the Boltzmann equation for N_1 is given

by :

$$\begin{aligned}
\frac{dY_{N_1}}{dz} = & \frac{2M_{pl}}{1.66 M_h^2} \frac{z\sqrt{g_*(z)}}{g_s(z)} \left(\langle \Gamma_{W^\pm \rightarrow e^\pm N_1} \rangle (Y_W^{eq} - Y_{N_1}) + \langle \Gamma_{Z_{BL} \rightarrow N_1 N_1} \rangle (Y_{Z_{BL}} - Y_{N_1}) \right. \\
& + \left. \sum_{i=H,h,Z} \langle \Gamma_{i \rightarrow N_1 N_1} \rangle (Y_i^{eq} - Y_{N_1}) \right) + \frac{4\pi^2}{45} \frac{M_{pl} M_h}{1.66} \frac{\sqrt{g_*(T)}}{z^2} \times \\
& \left(\sum_{x=W,Z,f,H} \langle \sigma_{v_{x\bar{x} \rightarrow N_1 N_1}} \rangle (Y_x^{eq\ 2} - Y_{N_1}^2) + \langle \sigma_{v_{Z_{BL} Z_{BL} \rightarrow N_1 N_1}} \rangle (Y_{Z_{BL}}^2 - Y_{N_1}^2) \right).
\end{aligned} \tag{28}$$

As discussed in Eq. (26), since the initial abundance of the sterile neutrino dark matter N_1 is very small, the Y_{N_1} term in the above equation may be neglected [23, 43]. Here $\langle \sigma_{v_{x\bar{x} \rightarrow N_1 N_1}} \rangle$ is the thermally averaged cross section for the production of N_1 from the annihilation of x particle. The expression of $\langle \sigma_{v_{x\bar{x} \rightarrow N_1 N_1}} \rangle$ is given by [59]⁵

$$\langle \sigma_{v_{x\bar{x} \rightarrow N_1 N_1}} \rangle = \frac{1}{8M_x^4 T K_2^2 \left(\frac{M_x}{T} \right)} \int_{4M_x^2}^{\infty} \sigma_{xx \rightarrow N_1 N_1} (s - 4M_x^2) \sqrt{s} K_1 \left(\frac{\sqrt{s}}{T} \right) ds. \tag{29}$$

The expressions for the relevant decay widths and annihilation cross sections are given in the Appendix A.1 and A.2 respectively.

In order to get the comoving number density (Y_{N_1}) of N_1 at the present epoch, we have to solve the coupled set of Boltzmann equations given in Eq. (26, 28). To be more precise, the value of $Y_{Z_{BL}}(z)$ for each z obtained by solving Eq. (26) is to be fed into Eq. (28). For understanding the physics behind this coupled set of Boltzmann equations better, let us first assume that the lightest sterile neutrinos are *only* produced from the decay of Z_{BL} , whereas Z_{BL} is produced and depleted according to Eq. (26). We plot the result in Fig. 2. In Fig. 2, initially at the early stage of the Universe there are no Z_{BL} particles and hence no N_1 , since for simplicity we have switched off all other production channels of N_1 , except Z_{BL} . Then, when Z_{BL} is produced from the decay of H , we also find an increase in the number density of N_1 from the decay of Z_{BL} . Finally, the number density of Z_{BL} begins to fall due to its dominating decay modes (production of Z_{BL} terminates as the the number density of H becomes negligibly small), and consequently the number density of N_1 also saturates since now there are no Z_{BL} left to aid the production of N_1 . This plot is also generated for the following chosen set of relevant parameters: $M_H = 500$ GeV, $M_{Z_{BL}} = 10$ GeV, $M_{N_1} = 1$ MeV and $g_{BL} = 10^{-10}$.

⁵As previously discussed, in a strict sense, one should use a definition of $\langle \sigma_{v_{Z_{BL} Z_{BL} \rightarrow N_1 N_1}} \rangle$ based on the non-equilibrium density function $f_{Z_{BL}}$.

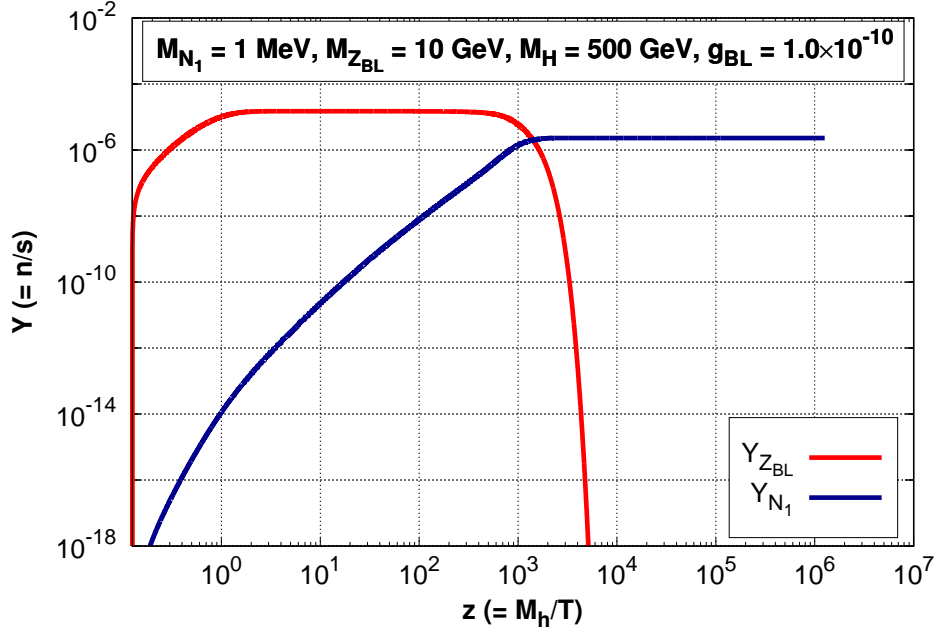


Figure 2: Evolution of comoving number densities of Z_{BL} and N_1 .

In Fig. 2 we have taken the initial temperature (T_i) to be 1 TeV. The final abundances of Z_{BL} and N_1 will not depend on this as long as $T_i \gtrsim M_H$. The maximum production of Z_{BL} from H decay occurs around a temperature of $\sim M_H$. However, if T_i becomes less than M_H then, since H is in thermal equilibrium, its own abundance will be exponentially suppressed (as it becomes non-relativistic) and thereby reducing $Y_{Z_{BL}}$ and Y_{N_1} . All these are shown in Fig. 3 where we see as discussed above, for $T_i \gtrsim M_H$, there is no change in the final values of $Y_{Z_{BL}}$ and Y_{N_1} (red, green, blue, cyan solid lines). While for $T_i \lesssim M_H$ both the final abundances are reduced (black solid line) from their previous values.

We now show the variation of Fig. 2 with different sets of chosen model parameters. In Fig. 4(a) we show the variation of $Y_{Z_{BL}}$ and Y_{N_1} with z for two different values of $U(1)_{B-L}$ gauge coupling g_{BL} . In this plot, we find that with increase in the value of g_{BL} the number density of Z_{BL} also increases initially. This is understandable, because the decay width $\Gamma_{H \rightarrow Z_{BL} Z_{BL}}$ increases with g_{BL} , and hence resulting in an increased number density of the extra gauge boson. But the depletion rate of Z_{BL} (proportional to its total decay width) also increases with g_{BL} , and hence will result in a faster fall of its comoving number density. This is also evident from the figure where the green line starts to fall earlier than the red one. On the other hand, the production rate of sterile neutrino dark matter (N_1) is proportional to $\Gamma_{Z_{BL} \rightarrow N_1 N_1}$ and $Y_{Z_{BL}}$ (see Eq. (28)) and both of these quantities increase with g_{BL} . Therefore, the comoving number density of N_1 increases as the value of g_{BL} changes from 1×10^{-10} to 5×10^{-10} .

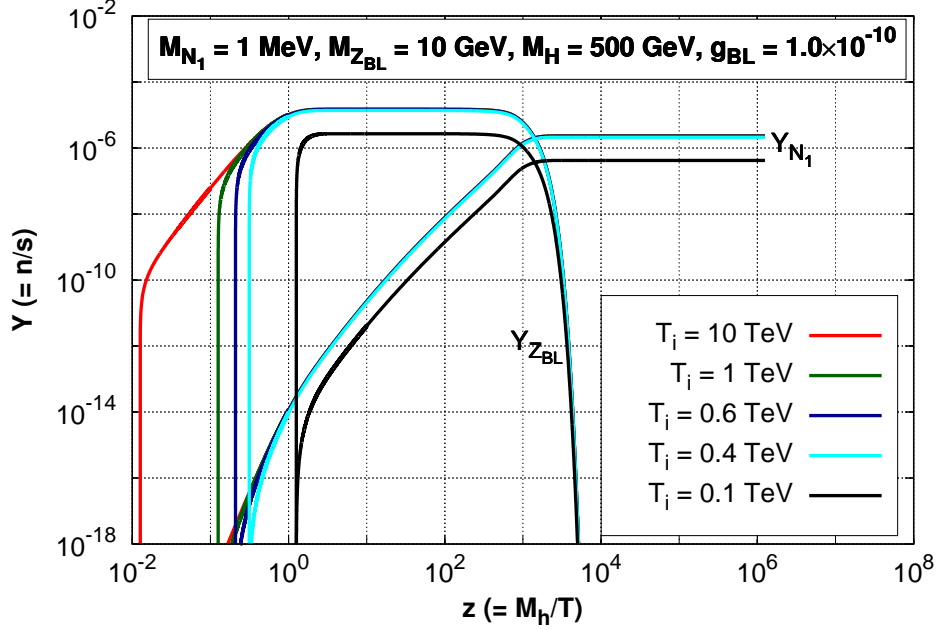


Figure 3: Dependence of $Y_{Z_{BL}}$ and Y_{N_1} on different sets of initial temperatures.

In Fig. 4(b), we show the variation of $Y_{Z_{BL}}$ and Y_{N_1} with z for two different values of M_H . Now, with a decrease in M_H , we expect a corresponding decrease in decay width $\Gamma_{H \rightarrow Z_{BL} Z_{BL}}$ (Z_{BL} production rate), and hence the initial number density of Z_{BL} will be smaller. This feature is seen in plot (b) where initially ($z \lesssim 10^3$) $Y_{Z_{BL}}$ for $M_H = 500$ GeV (green line) is larger than that for $M_H = 50$ GeV (red line). However, the total decay width of Z_{BL} (and consequently its depletion rate) does not depend on the mass of H . Hence both the red and green lines will start to fall off around the same time. Another noticeable change due to the variation of M_H is that the width of the “plateau” becomes narrower with the decrease in mass difference between M_H and $M_{Z_{BL}}$. Further, as the $Y_{Z_{BL}}$ increases with an increase in M_H , which in turn produces more N_1 (from the decay of Z_{BL}) in the final state and hence the comoving number density Y_{N_1} also increases with M_H .

In Fig. 4(c) we have shown the variation of $Y_{Z_{BL}}$ and Y_{N_1} for three different values of sterile neutrino dark matter mass. From this plot we find that there is not much variation in $Y_{Z_{BL}}$ with changing M_{N_1} . This is because the decay width $\Gamma_{Z_{BL} \rightarrow N_1 N_1}$ is subdominant with respect to the other decays modes of Z_{BL} . Increasing the mass of N_1 will lead to a further decrease of $\Gamma_{Z_{BL} \rightarrow N_1 N_1}$ and hence will not affect the depletion rate which is dominantly controlled by the other decay channels of Z_{BL} . But since in this case (when other production channels of N_1 are switched off) $\Gamma_{Z_{BL} \rightarrow N_1 N_1}$ solely controls the production rate of N_1 , Y_{N_1} changes with M_{N_1} . It is seen from Fig. 4(c) that if we increase the sterile neutrino mass from 1 MeV to 4 GeV (M_{N_1} tends to $M_{Z_{BL}}/2$),

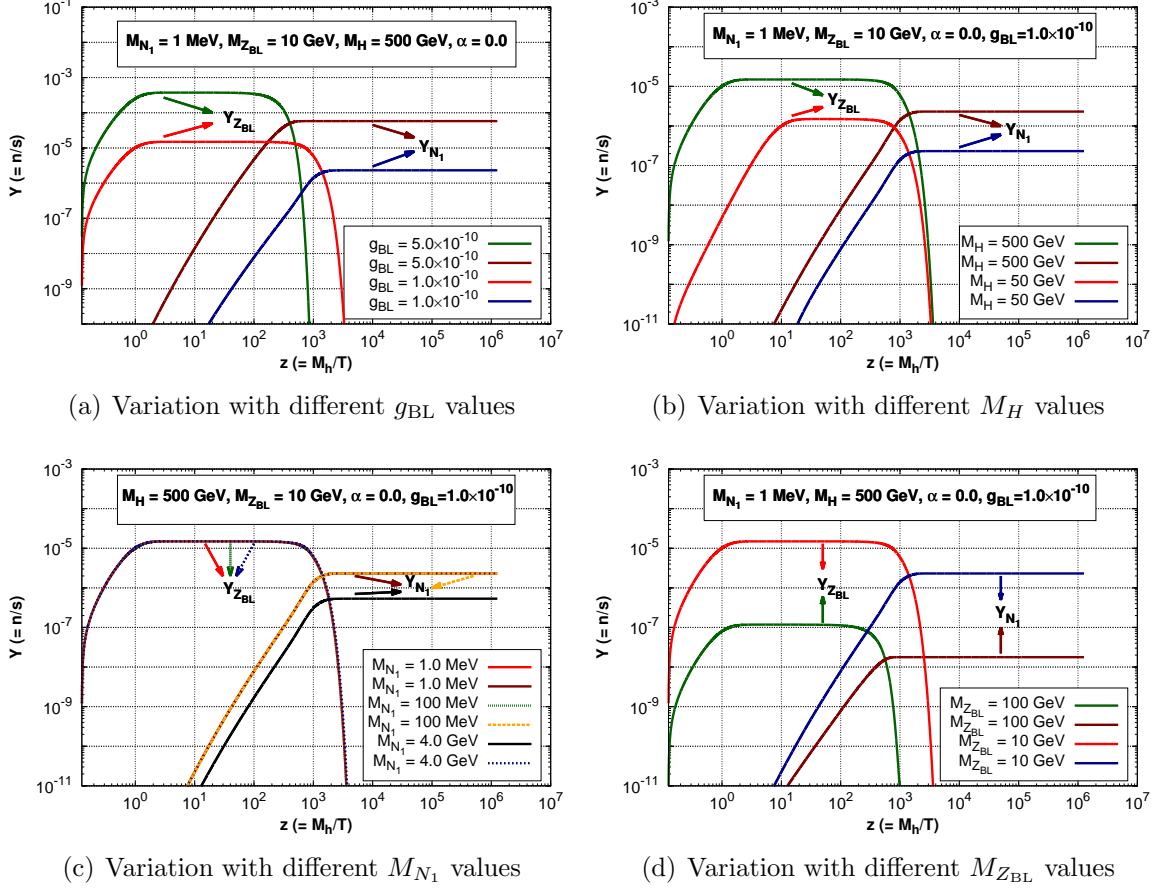


Figure 4: Comparison of comoving number densities of Z_{BL} and N_1 with respect to different sets of chosen model parameters.

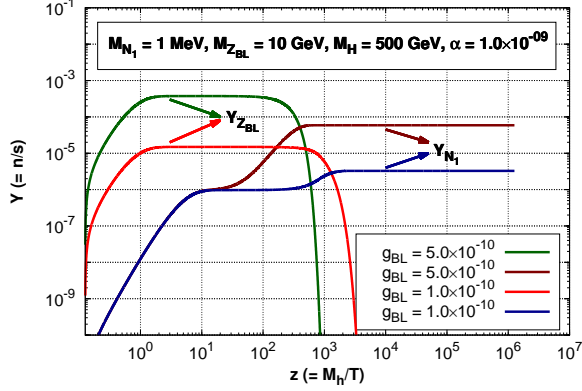
then Y_{N_1} decreases. The decrease in the decay width results in a corresponding decrease of Y_{N_1} as expected. However we find no visible change in Y_{N_1} when M_{N_1} goes from 1 MeV to 100 MeV. This is because in both of these cases $M_{Z_{BL}} \gg 2M_{N_1}$, therefore the decay width $\Gamma_{Z_{BL} \rightarrow N_1 N_1}$ and hence Y_{N_1} is practically insensitive to M_{N_1} ($M_{N_1} = 1$ MeV to 100 MeV).

Finally, the effect of the variation of gauge boson mass $M_{Z_{BL}}$ on $Y_{Z_{BL}}$ and Y_{N_1} is shown in Fig. 4(d). The increase in $M_{Z_{BL}}$ results in the decrease of $\Gamma_{H \rightarrow Z_{BL} Z_{BL}}$ and an increase of $\Gamma_{Z_{BL} \rightarrow all}$, which is manifested through a smaller rise and a faster fall of $Y_{Z_{BL}}$. This nature of $Y_{Z_{BL}}$ is corroborated in the plot as well, where $M_{Z_{BL}}$ varies from 10 GeV (red line) to 100 GeV (green line). On the other hand the quantity Y_{N_1} follows the evolution of $Y_{Z_{BL}}$ in the usual way as discussed earlier. Since all these cases were shown to demonstrate the validity of the coupled Boltzmann equations, for simplicity the active sterile mixing angle (α) is set to zero.

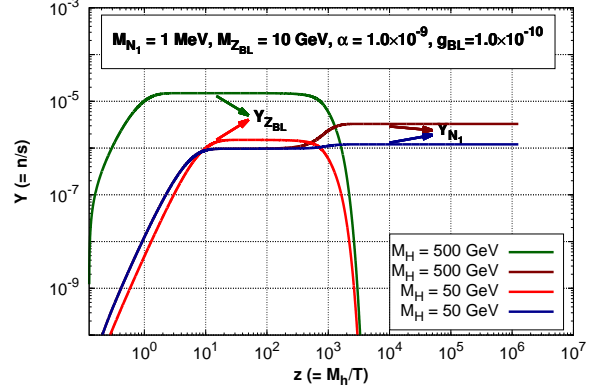
4.1 Solution of the complete Boltzmann equation(s) with all production and decay channels

In the previous section, we demonstrated the validity of the coupled set of Boltzmann equations needed to solve for the relic abundance of the sterile neutrino dark matter N_1 . For simplicity, we assumed that the only production channel of N_1 is the decay from Z_{BL} . However in general, all the possible production modes of N_1 including decays as well as annihilations of SM and BSM particles, as given in Eq. (28), have to be taken into account. Therefore, the active-sterile mixing angle is now nonzero. The noticeable feature when the active sterile mixing is nonzero is the production of N_1 from the decay of W^\pm bosons ($W^\pm \rightarrow e^\pm N_1$). It may a priori seem that due to small value of active-sterile mixing angle the contribution from the decay of W^\pm will be negligible, but we have to remember that in this non-thermal scenario, the extra gauge coupling (g_{BL}) is also required to be very small ($\sim 10^{-10}$), and hence the production of N_1 from the decay of Z_{BL} may also compete with the former. We will show this quantitatively later. Also note the decay of W^\pm is solely governed by the active-sterile mixing angle α and does not depend on $U(1)_{B-L}$ gauge coupling g_{BL} , hence if g_{BL} is made very low, the *only* dominant production channel of N_1 will be from W^\pm decay. In Fig. 5((a)-(d)) we show the variation Y_{N_1} and $Y_{Z_{BL}}$ with respect to different sets of independent parameters as before.

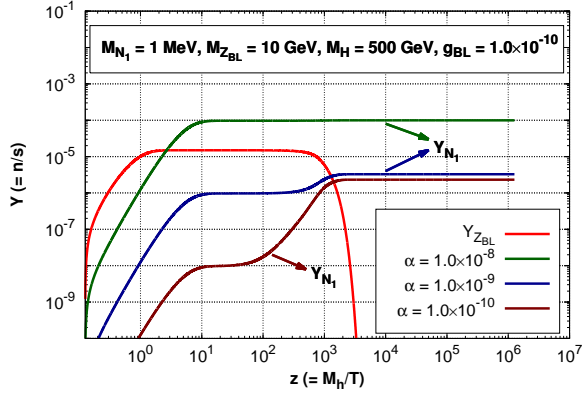
Interesting feature of Fig. 5((a)-(d)) when contrasted with Fig. 4((a)-(d)) is the existence of a “double plateau”. The reason behind this is the presence of another the production mode of N_1 from W^\pm decay which was neglected in previous section for simplicity. The onset of N_1 production as seen in these plots is a little early than those seen in Fig.4. The initial onset here is due to the presence of W^\pm decay and is independent of g_{BL} , $M_{Z_{BL}}$ and M_H (Eq. (33)), and only depends on α which is the sole parameter that controls the $W^\pm \rightarrow e^\pm N_1$ decay. The first plateau occurs when the number density of W boson begins to fall and hence there is a decreased rate of production of N_1 . However it again begins to rise sharply when the production from Z_{BL} starts to dominate. Then as before, we can see by comparing with the accompanying $Y_{Z_{BL}}$ lines that the second plateau results when the Z_{BL} number density starts to deplete. It is to be noted that this “two plateau” feature will be visible only when the production from W and Z_{BL} are comparable to each other at some point of $z(= \frac{M_h}{T})$. If either one of them remains dominant for all z , then it will result in single plateau like feature. For example, the green solid line in plot (c) of Fig. 5 has only a single plateau. This is because, due to a very high value of α the decay channels of W^\pm remain the most dominant production mode of N_1 for all z . The corresponding variation of Z_{BL} number density is also shown by red solid line and since α has no effect on the production and decay channels of Z_{BL} we find no variation of $Y_{Z_{BL}}$ with α . However the variation of Y_{N_1} is different for different values of α , as the active-sterile mixing angle α controls



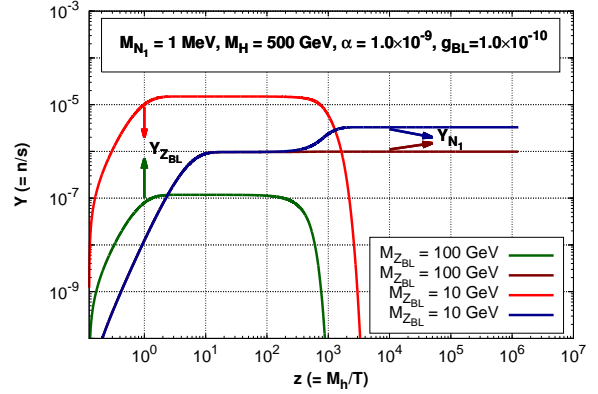
(a) Variation with different g_{BL} values



(b) Variation with different M_H values



(c) Variation with different α values



(d) Variation with different M_{ZBL} values

Figure 5: Comparison of Z_{BL} and N_1 comoving number density with respect to different sets of chosen parameters.

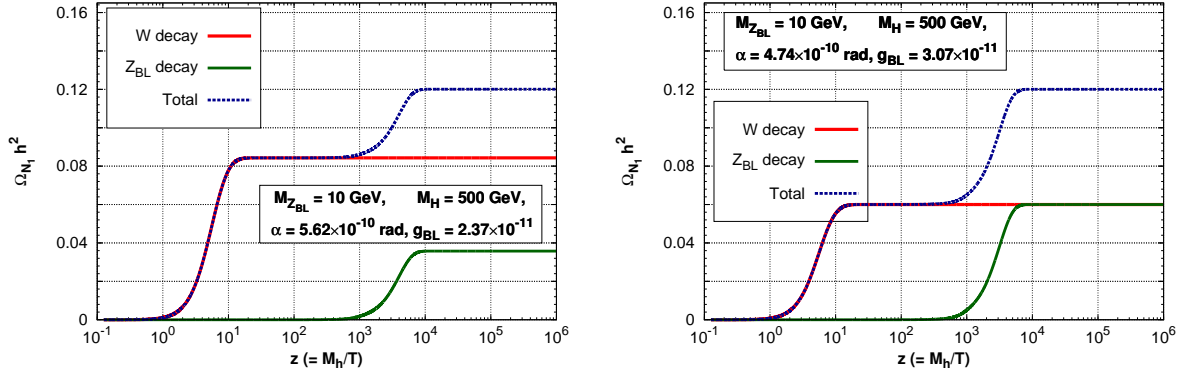
the production mode of N_1 from W^\pm decay.

5 Relic Density of Sterile Neutrino Dark Matter (N_1)

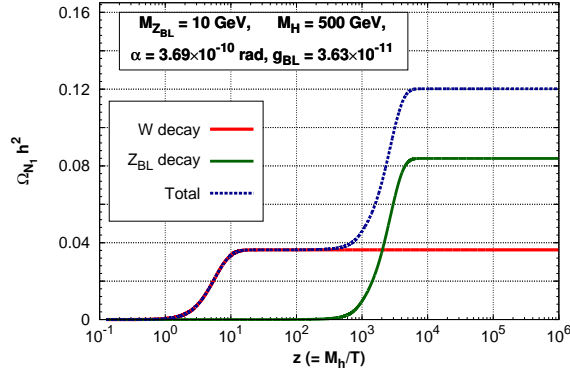
In order to compute the relic abundance ($\Omega_{N_1} h^2$) of the lightest sterile neutrino (N_1) we need to find the value of its comoving number density (Y_{N_1}) at the present epoch ($T = T_0$, $T_0 \sim 2.73$ K). The value of $Y_{N_1}(T_0)$ can be obtained by solving the two coupled Boltzmann equations (Eqs. (26, 28), which we have discussed elaborately in Section 4. The expression of $\Omega_{N_1} h^2$ in terms of $Y_{N_1}(T_0)$ is given by [68],

$$\Omega_{N_1} h^2 = 2.755 \times 10^8 \left(\frac{M_{N_1}}{\text{GeV}} \right) Y_{N_1}(T_0) . \quad (30)$$

In this work, we take all decay and annihilation channels of both SM as well as BSM particles for the production of N_1 . In Fig. 6 we show the relative contributions to $\Omega_{N_1} h^2$ from W^\pm (red solid line) and Z_{BL} decay (green solid line) for some chosen sets of model parameters. The total relic abundance of N_1 is also shown by the blue solid line. For some combinations of model parameters we find W^\pm decay can be the leading production channel of N_1 (plot (a)) while for some others it can be the subleading one (plot (c)). However in all three plots (a-c) of Fig. 6, the total relic density of N_1 has the saturation value ~ 0.12 which is in conformity with the value of dark matter relic density measured by the satellite borne experiment Planck. In plot (b) of



(a) W contribution to $\Omega_{N_1} h^2 \sim 70\%$ while Z_{BL} contribution $\sim 30\%$ (b) W contribution to $\Omega_{N_1} h^2 \sim Z_{BL}$ contribution



(c) W contribution to $\Omega_{N_1} h^2 \sim 30\%$ while Z_{BL} contribution $\sim 70\%$

Figure 6: Relic abundance of N_1 as function of z along with the relative contributions of W^\pm and Z_{BL} decay channels. All the plots are drawn for $M_{N_1} = 1$ MeV.

Fig. 6 we show a situation when the relative contributions to $\Omega_{N_1} h^2$ from both W^\pm and Z_{BL} decays are equal. In this case we have adopted the following values of relevant model parameters: $g_{BL} = 3.07 \times 10^{-11}$, $\alpha = 4.74 \times 10^{-10}$ rad, $M_{Z_{BL}} = 10$ GeV and $M_H = 500$ GeV. For this set of

model parameters we have also listed the fractional contributions to $\Omega_{N_1} h^2$ arising from all the possible decay and annihilation channels in Table 1, 2.

Decay Channel	Fractional contribution to $\Omega_{\text{DM}} h^2$
W^\pm	0.5000
Z_{BL}	0.4999
H	0.2590×10^{-10}
h	0.1177×10^{-11}
Z	0.6276×10^{-19}

Table 1: Fractional contributions of different production processes of N_1 through decay for $g_{\text{BL}} = 3.07 \times 10^{-11}$, $\alpha = 4.74 \times 10^{-10}$ rad, $M_{Z_{\text{BL}}} = 10$ GeV, $M_H = 500$ GeV and $M_{N_1} = 1$ MeV.

Annihilation Channel	Fractional contribution to $\Omega_{\text{DM}} h^2$
$t\bar{t}$	0.3745×10^{-12}
hh	0.1650×10^{-13}
W^+W^-	0.3606×10^{-14}
ZZ	0.3562×10^{-14}
HH	0.4403×10^{-19}
$Z_{\text{BL}}Z_{\text{BL}}$	0.4515×10^{-30}
$N_2\bar{N}_2$	0.1987×10^{-35}
$N_3\bar{N}_3$	0.1987×10^{-35}

Table 2: Fractional contributions of different production processes of N_1 through annihilation for $g_{\text{BL}} = 3.07 \times 10^{-11}$, $\alpha = 4.74 \times 10^{-10}$ rad, $M_{Z_{\text{BL}}} = 10$ GeV, $M_H = 500$ GeV and $M_{N_1} = 1$ MeV.

From Table 1 it is seen that for the small values of $g_{\text{BL}} \sim 10^{-11}$ and $\alpha \sim 10^{-10}$ (which are required for the non-thermality of N_1) the contributions of other production channels of N_1 through the decays of Z , H and h are negligible. Similarly, Table 2 shows that within this adopted ranges of model parameters the annihilation processes of SM as well as BSM particles do not contribute significantly to the production of sterile neutrino dark matter N_1 and hence we can safely consider the decays of W^\pm and Z_{BL} as the two most efficient production mechanisms of N_1 .

In Fig. 7, we plot the allowed values of B – L gauge coupling g_{BL} and active sterile mixing angle α which satisfy the relic density criteria ($0.1172 \leq \Omega_{N_1} h^2 \leq 0.1226$) [2]. During the computation of Fig. 7 we have varied the relevant parameters in the following range.

$$\begin{aligned} 0.1 \text{ GeV} &\leq M_{Z_{\text{BL}}} \leq 250 \text{ GeV} , \\ 1.2 \text{ MeV} &\leq M_{N_1} \leq 10 \text{ MeV} , \\ 10^{-8} &\leq g_{\text{BL}} \leq 10^{-15} , \\ 10^{-7} \text{ rad} &\leq \alpha \leq 10^{-17} \text{ rad} , \end{aligned} \tag{31}$$

and we have kept the mass of the extra Higgs boson H fixed at 500 GeV. From Fig. 7, we see that for very small values of the extra gauge coupling g_{BL} ($\sim 10^{-12}$ to 10^{-15}) the relic density condition of N_1 is always satisfied for a active-sterile mixing angle $\alpha \sim 10^{-10}$ rad. This is expected since for very small values of g_{BL} the production of N_1 from the decay of Z_{BL} is highly suppressed and in this situation decay of W^\pm becomes the principle production channel, since the latter is *not* suppressed by the extra gauge coupling (see Eqs. (33), (35)). Earlier works about the non-thermal production of sterile neutrino have not touched upon this point in detail (production of N_1 from W^\pm decay), since most of the previous authors have ignored the N_1 production mode from W^\pm decay in their works by assuming extremely small values of active-sterile mixing angle α . However, such an assumption needs careful attention when other couplings in the theory can also be very small. On the other hand for the higher values of g_{BL} ($\sim 10^{-9}$ to 10^{-11}) the decay of Z_{BL} becomes the dominant contributor and hence in this case small values of α are required to suppress the contribution of W^\pm decay to $\Omega_{N_1} h^2$ such that the total relic density of N_1 lies within the range prescribed by the Planck experiment. Since the production of sterile neutrino from W^\pm decay depends only on the mixing angle α , in Fig. 7 we get only a narrow band of α which satisfies the relic density of N_1 (for small values of g_{BL}). But when Z_{BL} is the main production channel of N_1 then for a given g_{BL} and α we can make N_1 to satisfy the relic density by adjusting the Z_{BL} mass. Hence we get a relatively wider band of allowed values of g_{BL} for a fixed α . For the chosen mass range of sterile neutrino (i.e. $\mathcal{O}(\text{MeV})$), from Fig. 7 we find that the maximum allowed value of α is $\sim 10^{-10}$ rad. Such a sterile neutrino is free from all the constraints arising from X-ray and BBN as seen from Fig. 1 of Ref. [24].

The allowed region in $M_{Z_{\text{BL}}} - g_{\text{BL}}$ plane is shown in Fig. 8. Like the previous plot in Fig. 7, here also all the points in $M_{Z_{\text{BL}}} - g_{\text{BL}}$ plane produce the correct relic density of N_1 ($0.1172 \leq \Omega_{N_1} h^2 \leq 0.1226$). In this case we have also varied the other relevant parameters (M_{N_1}, α) in the range given in Eq. (31). From this figure it is seen that the allowed values of g_{BL} increases with $M_{Z_{\text{BL}}}$. This nature of $M_{Z_{\text{BL}}} - g_{\text{BL}}$ plane can be explained in the following way. We know that the contribution of Z_{BL} to Y_{N_1} depends on both $\Gamma_{Z_{\text{BL}} \rightarrow N_1 N_1}$ and $Y_{Z_{\text{BL}}}$ (see Eq. (28)) where the latter quantity increases with $\Gamma_{H \rightarrow Z_{\text{BL}} Z_{\text{BL}}}$ (Eq. (26)) as the extra gauge bosons Z_{BL} are produced

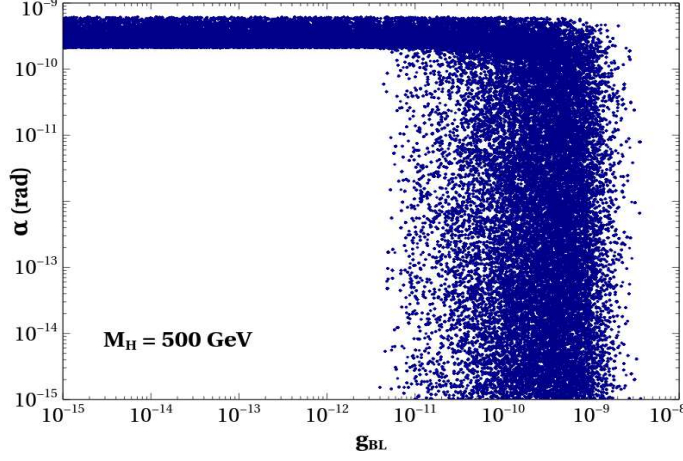


Figure 7: Allowed region in g_{BL} Vs α plane satisfying the relic density criteria.

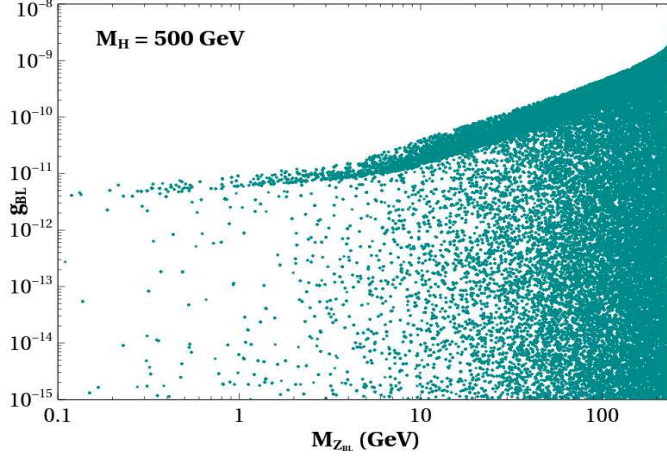


Figure 8: Allowed region in $M_{Z_{BL}}$ Vs g_{BL} plane satisfying the relic density criteria.

mainly from the decay of H . However the decay width $\Gamma_{H \rightarrow Z_{BL} Z_{BL}}$ is suppressed by $M_{Z_{BL}}^{-2}$ and thereby reducing the comoving number density of Z_{BL} with its mass (see Eq. (55) and Fig. 5(d)). In order to keep the contribution to $\Omega_{N_1} h^2$ arising from Z_{BL} decay unaltered, this decrement in $Y_{Z_{BL}}$ must be compensated by a corresponding increment in $\Gamma_{Z_{BL} \rightarrow N_1 N_1}$ which is proportional to g_{BL}^2 (Eq. (35)). Hence with an increase in $M_{Z_{BL}}$, g_{BL} should also increase to satisfy the relic density constraint.

Simulations using the standard Λ CDM cosmology requires that most of the dark matter candidates should be *cold* to satisfy constraints from the structure formation [69, 70]. In our case, to get an idea about the *coldness* of the sterile neutrino dark matter we try to compute its

free-streaming length defined by [63]:

$$\lambda_{\text{fs}} = \int_{t_{\text{in}}}^{t_0} \frac{\langle v(t) \rangle}{a(t)} dt,$$

where t_{in} is the initial time, t_0 is the present time, $v(t)$ is the mean velocity of the dark matter, and $a(t)$ is the scale factor of the Universe. Following Ref. [43], the hot, cold and warm dark matters are classified as:

$$\begin{aligned} \text{Cold Dark Matter (CDM)} & : \lambda_{\text{fs}} < 0.01 \text{ Mpc} \\ \text{Warm Dark Matter (WDM)} & : 0.01 \text{ Mpc} < \lambda_{\text{fs}} < 0.1 \text{ Mpc} \\ \text{Hot Dark Matter (HDM)} & : \lambda_{\text{fs}} > 0.1 \text{ Mpc} \end{aligned}$$

For the case where both W^\pm and Z_{BL} contribute equally to the final dark matter relic density (Fig. 6b), we have calculated the free-streaming length for dark matter produced from W^\pm as well as Z_{BL} decay separately. In both the cases we find that $\lambda_{\text{fs}}^{W^\pm} \sim 0.003 \text{ Mpc}$ and $\lambda_{\text{fs}}^{Z_{\text{BL}}} \sim 0.007 \text{ Mpc}$. Hence following the above classification of hot, cold and warm dark matter, we find that all of our sterile neutrino is *cold* and thus satisfying the structure formation constraints.

6 A possible way of detecting the sterile neutrino Dark Matter

In 2003 INTEGRAL/SPI [50] of ESA observed an emission line at an energy of 511 keV mostly from the galactic bulge. Recently, it has been reported that the measured flux from the galactic bulge by INTEGRAL/SPI is $\Phi_{511}^{\text{exp}} = (0.96 \pm 0.07) \times 10^{-3} \text{ ph cm}^{-2} \text{ s}^{-1}$ at 56σ significance [71]. A possible source of this line is assumed to be the annihilation of electron and positron in the galactic core. In spite of some astrophysical processes explaining the origin of the line [72], the sources of the galactic positrons are not clear yet. Hence a series of possible explanations have been reported in last ten years involving positrons originating from a decaying [73, 74] or annihilating [75, 76] dark matter. For a brief review of earlier works trying to explain 511 keV line see [77]. Recently the authors of Ref. [78] have shown that the explanation of this anomalous emission line is not possible from the annihilation of thermal dark matter (WIMP) due to conflict with the latest cosmological data and they have preferred a non-thermal origin of dark matter for explaining this long standing puzzle. Earlier people have tried to explain this INTEGRAL anomaly from the decay of light sterile neutrino dark matter [79, 49]. Here, in the case of sterile neutrino dark matter in a non-thermal setting, we have also found that such an explanation is indeed possible. The decaying dark matter scenarios however require a more cuspy density profile

than the annihilation models [80]. The seed mechanism behind this 511 keV emission line is the decay of sterile neutrino (N_1) into a e^\pm pair and an active neutrino. The e^\pm pair thus produced, get slowed down to non relativistic velocities due to several energy loss mechanisms within the galactic bulge [81] and thereby producing 511 keV *gamma-line* from their pair annihilation. The mass of the sterile neutrino favourable to explain this signal is $\sim 1\text{-}10$ MeV [81]. In the present $U(1)_{B-L}$ model, there are six possible Feynman diagrams contributing to this three body decay of which those which are mediated by Z_{BL} , h and H are sub dominant due to the suppression by the very low value of $U(1)_{B-L}$ gauge coupling g_{BL} . Therefore, we have used the remaining three diagrams i.e. those mediated by Z and W^\pm bosons to calculate the three body decay width. The expression of matrix amplitude squared and corresponding decay width $\Gamma_{N_1 \rightarrow e^\pm \nu}$ is given in Appendix A.4. A more simpler analytical expression (using some approximation) for this three body decay width can be found in Ref. [79]. The expression for the gamma ray flux obtained from the galactic bulge due the decay $N_1 \rightarrow e^\pm \nu$ is given by [79]:

$$\Phi_{511}^{theory} = 2 \frac{1}{4\pi} \frac{\Gamma_{N_1 \rightarrow e^\pm \nu}}{M_{N_1}} \frac{\int_{\Delta\Omega} \int_{l.o.s} \rho_{DM}(r(s, \Omega)) ds d\Omega}{\int_{\Delta\Omega} d\Omega}. \quad (32)$$

Here, $\Gamma_{N_1 \rightarrow e^\pm \nu}$ is the decay width of $N_1 \rightarrow e^\pm \nu$ and $\rho_{DM}(s, \Delta\Omega)$ is the dark matter density profile in the galaxy. During our analysis, we have taken Einasto profile [82] with $\alpha_{einasto} = 0.17$ for the computation of gamma-ray flux. The angular integration over the solid angle $\Delta\Omega$ is performed within the 2° angular resolution of the spectrometer while the spacial integration is over the line of sight (l.o.s) distance of galactic bulge from the position of solar system. The extra factor of 2 appearing in Eq. (32) is due to the production of two photons per decay of N_1 .

Using Eq. (32) we have computed the photon flux for different values of M_{N_1} and α . In Fig. (9) the red band shows the correct combination of M_{N_1} and α which is needed to explain the INTEGRAL observed flux. The dark cyan region is for those values of M_{N_1} and α which satisfies only the relic density constraint of N_1 . From Fig. 9, we can see that in the chosen range of M_{N_1} ($\sim 1 - 10$ MeV) the active-sterile mixing angle α required to explain *both* the relic density as well as the INTEGRAL anomaly is $\sim 10^{-12} - 10^{-14}$ rad.

7 Conclusion

In this work we have shown that non-thermal sterile neutrino in $U(1)_{B-L}$ model can be a viable dark matter candidate. But the formalism developed here is in general applicable to any $U(1)_X$ extension of the Standard Model. Any such model trying to describe a non-thermal dark matter scenario (through IR Freeze-in) will have in general a very weakly coupled Z' as well as a feebly

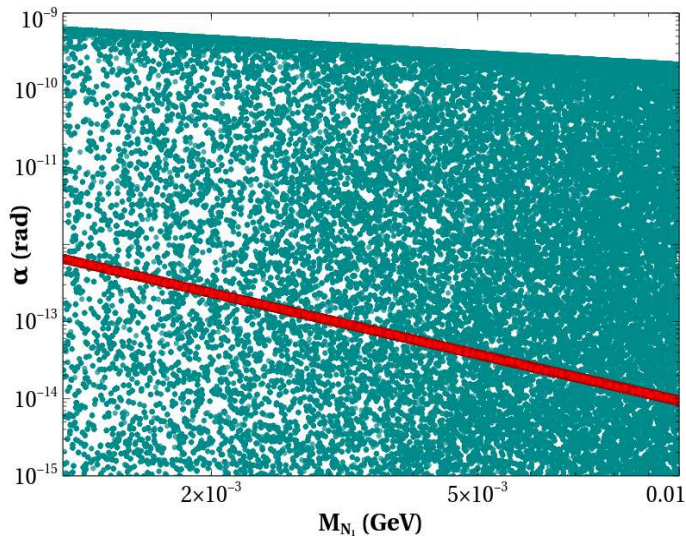


Figure 9: Values of M_{N_1} and active-sterile mixing angle α allowed by the relic density of N_1 ($0.1172 \leq \Omega_{N_1} h^2 \leq 0.1226$), are shown by the dark cyan points. The points lying within the red coloured band reproduced the flux observed by INTEGRAL/SPI.

coupled dark matter candidate. Under such circumstances (i.e. when the mother particle responsible for most of the production of the dark matter has itself gone out of thermal equilibrium), we have shown how to solve a set of coupled Boltzmann equations to calculate the final relic density. We have seen that the sterile neutrinos are mostly produced from the decay of Z_{BL} and W^\pm . We have also shown that though the contribution from W^\pm was neglected in the previous works (under the assumption of smallness of the active-sterile mixing angle), it can actually be sizeable (even dominating over the production from Z_{BL} decay for some values of α and g_{BL}) depending on the parameter space we are focussing on. Note that for generic values of α we use in this work, one of the active neutrinos has to be very light. However this is allowed by the data available from the various present day neutrino experiments. Finally for completeness, we have also checked that such an $\mathcal{O}(\text{MeV})$ mass non-thermal sterile neutrino can explain the 511 keV line observed by INTEGRAL/SPI. The α required to explain this signal falls in the region where the dark matter production is mostly dominated by Z_{BL} decay. The decay width required has a corresponding life time $\sim 10^{25}$ s, which much larger than the present age of the Universe ($\sim 10^{17}$ s).

8 Acknowledgement

Authors would like to thank Raj Gandhi, Alexander Merle, Sourav Mitra, Tirthankar Roy Choudhury, Osamu Seto and Bibhushan Shakya for many useful suggestions and discussions. Authors would also like to thank Mehedi Masud, Avirup Shaw and Taushif Ahmed for helping out with various aspects of numerical calculations. Authors also acknowledge Department of Atomic Energy (DAE), Govt. of India for their financial assistance and the cluster computing facility at HRI (<http://cluster.hri.res.in>).

A Analytical expressions for cross sections and decay widths

A.1 Production processes of N_1 from the decays of SM and BSM particles

In this section, we give the expressions of all the relevant decay widths which are needed to solve the coupled Boltzmann equation for N_1 (Eqs. (28)).

$$\Gamma(W^+ \rightarrow N_1 e^+) = \frac{2(2M_W^4 - (M_e^2 - M_{N_1}^2)^2 - (M_e^2 + M_{N_1}^2)M_W^2) \sin^2 \alpha}{3v^2} \times \frac{\sqrt{1 - \left(\frac{M_e + M_{N_1}}{M_W}\right)^2} \sqrt{1 - \left(\frac{M_e - M_{N_1}}{M_W}\right)^2}}{16\pi M_W}, \quad (33)$$

$$\Gamma(Z \rightarrow N_1 \bar{N}_1) = \frac{M_Z^3 \sin^4 \alpha}{24\pi v^2} \left(1 - \frac{4M_{N_1}^2}{M_Z^2}\right)^{3/2}, \quad (34)$$

$$\Gamma(Z_{\text{BL}} \rightarrow N_1 \bar{N}_1) = \frac{M_{Z_{\text{BL}}}^3}{24\pi} ((\sin^2 \alpha - \cos^2 \alpha)^2 g_{\text{BL}}^2) \left(1 - \frac{4M_{N_1}^2}{M_{Z_{\text{BL}}}^2}\right)^{3/2}, \quad (35)$$

$$\Gamma(H \rightarrow N_1 \bar{N}_1) = \frac{g_{HN_1 N_1}^2 M_H}{16\pi} \left(1 - \frac{4M_{N_1}^2}{M_H^2}\right)^{3/2}, \quad (36)$$

$$\Gamma(h \rightarrow N_1 \bar{N}_1) = \frac{g_{hN_1 N_1}^2 M_h}{16\pi} \left(1 - \frac{4M_{N_1}^2}{M_h^2}\right)^{3/2}, \quad (37)$$

where M_x denotes the mass of particle x , α is the active-sterile mixing angle of first generation (i.e. mixing of ν_1 with N_1) while $g_{HN_1 N_1}$ and $g_{hN_1 N_1}$ are vertex factors corresponding to the vertices $HN_1 N_1$ and $hN_1 N_1$ respectively. With respect to our chosen set of independent

parameters, these vertex factors are given as:

$$\begin{aligned}
g_{HN_1N_1} &= 2 \cos \alpha \left(\sin \theta \sin \alpha \frac{\sqrt{M_{N_1} m_{\nu_1}}}{v} - \cos \theta \cos \alpha \frac{g_{\text{BL}} M_{N_1}}{M_{Z_{\text{BL}}}} \right), \\
g_{hN_1N_1} &= 2 \cos \alpha \left(\cos \theta \sin \alpha \frac{\sqrt{M_{N_1} m_{\nu_1}}}{v} + \sin \theta \cos \alpha \frac{g_{\text{BL}} M_{N_1}}{M_{Z_{\text{BL}}}} \right).
\end{aligned} \tag{38}$$

A.2 Production processes of N_1 from annihilation

In this section, we present the expressions of all the relevant annihilation cross sections i.e. the production processes of N_1 through the annihilations of SM as well as BSM particles. In all the expressions given below, M_X and Γ_X denote the mass and total decay width of the particle X while g_{ijk} denotes the coupling of the vertex involving fields i, j, k . Further, \sqrt{s} is the center of mass energy of a particular annihilation process. All the annihilation cross sections given below are written in terms of our chosen set of independent parameters.

$$\underline{\mathbf{W}^+ \mathbf{W}^- \rightarrow \mathbf{N}_1 \bar{\mathbf{N}}_1}$$

In this annihilation process, three s -channel diagrams mediated by h , H and Z and one electron mediated t -channel diagram are possible. However, Z boson and electron mediated diagrams are suppressed respectively by the fourth and second power of the active-sterile mixing angle α . Therefore we have considered other two s -channel diagrams only.

$$\begin{aligned}
g_{WW h} &= \frac{2M_W^2}{v} \cos \theta, \\
g_{WW H} &= \frac{2M_W^2}{v} \sin \theta, \\
A_{WW} &= \frac{g_{WW h} g_{hN_1N_1} ((s - M_h^2) - i M_h \Gamma_h)}{(s - M_h^2)^2 + (M_h \Gamma_h)^2} + \frac{g_{WW H} g_{HN_1N_1} ((s - M_H^2) - i M_H \Gamma_H)}{(s - M_H^2)^2 + (M_H \Gamma_H)^2}, \\
|M_{WW}|^2 &= \frac{4}{9} (s - 4M_{N_1}^2) \left(1 + \frac{(s - 2M_W^2)^2}{8M_W^4} \right) |A_{WW}|^2, \\
\sigma_{WW} &= \frac{1}{32\pi s} \frac{\sqrt{1 - \frac{4M_{N_1}^2}{s}}}{\sqrt{1 - \frac{4M_W^2}{s}}} |M_{WW}|^2.
\end{aligned} \tag{39}$$

$ZZ \rightarrow N_1 \bar{N}_1$

There are two s -channel diagrams and two t -channel diagrams for $ZZ \rightarrow N_1 \bar{N}_1$ annihilation process. The t -channel diagrams mediated by active and sterile neutrinos are suppressed by fourth and eighth power of α respectively. Hence we have considered only two s -channel diagrams mediated by h and H .

$$\begin{aligned}
g_{ZZh} &= \frac{2M_Z^2}{v} \cos \theta, \\
g_{ZZH} &= \frac{2M_Z^2}{v} \sin \theta, \\
A_{ZZ} &= \frac{g_{ZZh} g_{hN_1 N_1} ((s - M_h^2) - i M_h \Gamma_h)}{(s - M_h^2)^2 + (M_h \Gamma_h)^2} + \frac{g_{ZZH} g_{HN_1 N_1} ((s - M_H^2) - i M_H \Gamma_H)}{(s - M_H^2)^2 + (M_H \Gamma_H)^2}, \\
|M_{ZZ}|^2 &= \frac{4}{9} (s - 4M_{N_1}^2) \left(1 + \frac{(s - 2M_Z^2)^2}{8M_Z^4} \right) |A_{ZZ}|^2, \\
\sigma_{ZZ} &= \frac{1}{32\pi s} \frac{\sqrt{1 - \frac{4M_{N_1}^2}{s}}}{\sqrt{1 - \frac{4M_Z^2}{s}}} |M_{ZZ}|^2. \tag{40}
\end{aligned}$$

$f\bar{f} \rightarrow N_1 \bar{N}_1$ (where f denotes any SM quarks or leptons)

In this annihilation process four s -channel diagrams, mediated by Z , Z_{BL} , h and H , are possible. However, the Z boson mediated diagram is suppressed by α^4 and consequently we have neglected it.

$$\begin{aligned}
g_{ffh} &= -\frac{M_f}{v} \cos \theta, \\
g_{ffH} &= -\frac{M_f}{v} \sin \theta, \\
A_{ff} &= \frac{g_{ffh} g_{hN_1 N_1} ((s - M_h^2) - i M_h \Gamma_h)}{(s - M_h^2)^2 + (M_h \Gamma_h)^2} + \frac{g_{ffH} g_{HN_1 N_1} ((s - M_H^2) - i M_H \Gamma_H)}{(s - M_H^2)^2 + (M_H \Gamma_H)^2}, \\
|M_{ff}|^2 &= \frac{g_{BL}^4 q_f^2 \left(\frac{8(s - 4M_{N_1}^2)(s + 2M_f^2)}{3n_c} \right)}{(s - M_{Z_{BL}}^2)^2 + (\Gamma_{Z_{BL}} M_{Z_{BL}})^2} + \frac{2}{n_c} |A_{ff}|^2 (s - 4M_{N_1}^2)(s - 4M_f^2) \\
\sigma_{ff} &= \frac{1}{64\pi s} \frac{\sqrt{1 - \frac{4M_{N_1}^2}{s}}}{\sqrt{1 - \frac{4M_f^2}{s}}} |M_{ff}|^2, \tag{41}
\end{aligned}$$

where n_c is the colour charge of the corresponding fermion (f).

Although, the annihilation processes $HH \rightarrow N_1 \bar{N}_1$, $hh \rightarrow N_1 \bar{N}_1$ consist of two t -channel and two s -channel diagrams, we consider only the two dominant s -channel diagrams mediated by H and h .

$HH \rightarrow N_1 \bar{N}_1$

$$\begin{aligned}
g_{HHh} &= 2 \sin \theta \cos^2 \theta (3\lambda_2 - \lambda_3) v_{\text{BL}} - \lambda_3 v \cos^3 \theta + 2 \cos \theta \sin^2 \theta (\lambda_3 - 3\lambda_1) v + \lambda_3 v_{\text{BL}} \sin^3 \theta, \\
g_{HHH} &= -3 (\lambda_3 \sin \theta \cos^2 \theta v + 2 \cos^3 \theta \lambda_2 v_{\text{BL}} + \sin^2 \theta \cos \theta \lambda_3 v_{\text{BL}} + 2 \sin^3 \theta \lambda_1 v), \\
A_{HH} &= \frac{g_{HHh} g_{hN_1 N_1} ((s - M_h^2) - i M_h \Gamma_h)}{(s - M_h^2)^2 + (M_h \Gamma_h)^2} + \frac{g_{HHH} g_{HN_1 N_1} ((s - M_H^2) - i M_H \Gamma_H)}{(s - M_H^2)^2 + (M_H \Gamma_H)^2}, \\
|M_{HH}|^2 &= 2 (s - 4M_{N_1}^2) |A_{ZZ}|^2, \\
\sigma_{HH} &= \frac{1}{32\pi s} \frac{\sqrt{1 - \frac{4M_{N_1}^2}{s}}}{\sqrt{1 - \frac{4M_H^2}{s}}} |M_{HH}|^2.
\end{aligned} \tag{42}$$

$hh \rightarrow N_1 \bar{N}_1$

$$\begin{aligned}
g_{hhH} &= 2 \sin \theta \cos^2 \theta (\lambda_3 - 3\lambda_1) v - \lambda_3 v_{\text{BL}} \cos^3 \theta + 2 \cos \theta \sin^2 \theta (\lambda_3 - 3\lambda_2) v_{\text{BL}} - \lambda_3 v \sin^3 \theta, \\
g_{hhh} &= 3 (\lambda_3 \sin \theta \cos^2 \theta v_{\text{BL}} - 2 \cos^3 \theta \lambda_1 v - \sin^2 \theta \cos \theta \lambda_3 v + 2 \sin^3 \theta \lambda_2 v_{\text{BL}}), \\
A_{hh} &= \frac{g_{hhh} g_{hN_1 N_1} ((s - M_h^2) - i M_h \Gamma_h)}{(s - M_h^2)^2 + (M_h \Gamma_h)^2} + \frac{g_{hhH} g_{HN_1 N_1} ((s - M_H^2) - i M_H \Gamma_H)}{(s - M_H^2)^2 + (M_H \Gamma_H)^2}, \\
|M_{hh}|^2 &= 2 (s - 4M_{N_1}^2) |A_{hh}|^2, \\
\sigma_{hh} &= \frac{1}{32\pi s} \frac{\sqrt{1 - \frac{4M_{N_1}^2}{s}}}{\sqrt{1 - \frac{4M_h^2}{s}}} |M_{hh}|^2.
\end{aligned} \tag{43}$$

$\lambda_1, \lambda_2, \lambda_3$ has been previously expressed in terms of the independent parameters (Eqs. (19-21)).

$$\underline{\mathbf{Z}_{\text{BL}} \mathbf{Z}_{\text{BL}} \rightarrow \mathbf{N}_1 \bar{\mathbf{N}}_1}$$

This annihilation process is also mediated by two s -channel diagrams and two t -channel diagrams. However the t -channel diagram mediated by active neutrino is suppressed by α^4 . Therefore we have considered two s -channel diagrams and one t -channel diagram mediated by H , h and N_1 respectively. For simplicity, due to smallness of α , we have considered $\cos \alpha \simeq 1$ and consequently $\sin \alpha \simeq 0$ in the following expressions (Eq. (44)-(51)).

$$\begin{aligned}
A_1 = & \left[-2g_{\text{BL}}^4 \left(- (4M_{N_1}^2 - s)^{3/2} (4M_{\text{ZBL}}^2 - s)^{3/2} \left(s^2 M_{\text{ZBL}}^4 + 20s M_{\text{ZBL}}^6 - 48M_{\text{ZBL}}^8 + \right. \right. \right. \\
& 2M_{N_1}^4 (-56s M_{\text{ZBL}}^2 + 16M_{\text{ZBL}}^4 + s^2) + M_{N_1}^2 (16s^2 M_{\text{ZBL}}^2 - 102s M_{\text{ZBL}}^4 + 184M_{\text{ZBL}}^6 + s^3) \left. \left. \left. \right) \right. \right. \\
& + 12M_{\text{ZBL}}^4 (2M_{\text{ZBL}}^2 - 8M_{N_1}^2 - s) (M_{N_1}^2 (s - 4M_{\text{ZBL}}^2) + M_{\text{ZBL}}^4) \\
& \left. \left. 2(s - 4M_{\text{ZBL}}^2)(4M_{N_1}^2 - s) \log \left(\frac{s - \sqrt{4M_{N_1}^2 - s} \sqrt{4M_{\text{ZBL}}^2 - s} - 2M_{\text{ZBL}}^2}{s + \sqrt{4M_{N_1}^2 - s} \sqrt{4M_{\text{ZBL}}^2 - s} - 2M_{\text{ZBL}}^2} \right) \right) \right] \times \\
& \frac{1}{27M_{\text{ZBL}}^4 (4M_{N_1}^2 - s)^{3/2} (4M_{\text{ZBL}}^2 - s)^{3/2} (M_{N_1}^2 (s - 4M_{\text{ZBL}}^2) + M_{\text{ZBL}}^4)}, \tag{44}
\end{aligned}$$

$$\begin{aligned}
A_2 = & \left[\sqrt{4M_{N_1}^2 - s} (2M_{\text{ZBL}}^2 - s) \sqrt{4M_{\text{ZBL}}^2 - s} \left(M_{N_1}^2 (88M_{\text{ZBL}}^2 - 46s) + s (20M_{\text{ZBL}}^2 + s) \right) + \right. \\
& 48s (M_{N_1} - M_{\text{ZBL}}) (M_{\text{ZBL}} + M_{N_1}) (M_{N_1}^2 (4M_{\text{ZBL}}^2 - s) - M_{\text{ZBL}}^4) \times \\
& \left. \log \left(\frac{1 + \frac{\sqrt{4M_{N_1}^2 - s} (s - 2M_{\text{ZBL}}^2) \sqrt{4M_{\text{ZBL}}^2 - s}}{M_{N_1}^2 (8M_{\text{ZBL}}^2 - 2s) - 4s M_{\text{ZBL}}^2 + 2M_{\text{ZBL}}^4 + s^2}}{1 - \frac{\sqrt{4M_{N_1}^2 - s} (s - 2M_{\text{ZBL}}^2) \sqrt{4M_{\text{ZBL}}^2 - s}}{M_{N_1}^2 (8M_{\text{ZBL}}^2 - 2s) - 4s M_{\text{ZBL}}^2 + 2M_{\text{ZBL}}^4 + s^2}} \right) \right] \frac{2g_{\text{BL}}^4}{27M_{\text{ZBL}}^4 \sqrt{4M_{N_1}^2 - s} (s - 2M_{\text{ZBL}}^2) \sqrt{4M_{\text{ZBL}}^2 - s}}, \tag{45}
\end{aligned}$$

$$\begin{aligned}
A_3 = & \left[\left(\sqrt{s - 4M_{N_1}^2} \sqrt{s - 4M_{Z_{BL}}^2} (-2sM_{Z_{BL}}^2 + 4M_{Z_{BL}}^4 + s^2) \right. \right. \\
& + 2 \left(M_{N_1}^2 (-4sM_{Z_{BL}}^2 + 8M_{Z_{BL}}^4 + s^2) - 2M_{Z_{BL}}^6 \right) \times \\
& \left. \log \left(\frac{s - \sqrt{s - 4M_{N_1}^2} \sqrt{s - 4M_{Z_{BL}}^2} - 2M_{Z_{BL}}^2}{s + \sqrt{s - 4M_{N_1}^2} \sqrt{s - 4M_{Z_{BL}}^2} - 2M_{Z_{BL}}^2} \right) \right) \\
& \left. 64 g_{BL}^4 \sin^2 \theta M_{N_1}^2 (M_h^2 - s) \right] \times \\
& \frac{1}{9M_{Z_{BL}}^4 \sqrt{s - 4M_{N_1}^2} \sqrt{s - 4M_{Z_{BL}}^2} (\Gamma_h^2 M_h^2 + (M_h^2 - s)^2)}, \tag{46}
\end{aligned}$$

$$\begin{aligned}
A_4 = & \left[\left(\sqrt{s - 4M_{N_1}^2} \sqrt{s - 4M_{Z_{BL}}^2} (-2sM_{Z_{BL}}^2 + 4M_{Z_{BL}}^4 + s^2) \right. \right. \\
& + 2 \left(M_{N_1}^2 (-4sM_{Z_{BL}}^2 + 8M_{Z_{BL}}^4 + s^2) - 2M_{Z_{BL}}^6 \right) \times \\
& \left. \log \left(\frac{s - \sqrt{s - 4M_{N_1}^2} \sqrt{s - 4M_{Z_{BL}}^2} - 2M_{Z_{BL}}^2}{s + \sqrt{s - 4M_{N_1}^2} \sqrt{s - 4M_{Z_{BL}}^2} - 2M_{Z_{BL}}^2} \right) \right) \\
& \left. 64 g_{BL}^4 \cos^2 \theta M_{N_1}^2 (M_H^2 - s) \right] \times \\
& \frac{1}{9M_{Z_{BL}}^4 \sqrt{s - 4M_{N_1}^2} \sqrt{s - 4M_{Z_{BL}}^2} (\Gamma_H^2 M_H^2 + (M_H^2 - s)^2)}, \tag{47}
\end{aligned}$$

$$A_5 = \frac{32 g_{BL}^4 \sin^4 \theta M_{N_1}^2 (s - 4M_{N_1}^2) (s^2 - 4sM_{Z_{BL}}^2 + 12M_{Z_{BL}}^4)}{9 M_{Z_{BL}}^4 (\Gamma_h^2 M_h^2 + (M_h^2 - s)^2)}, \tag{48}$$

$$A_6 = \frac{32 g_{BL}^4 \cos^4 \theta M_{N_1}^2 (s - 4M_{N_1}^2) (s^2 - 4sM_{Z_{BL}}^2 + 12M_{Z_{BL}}^4)}{9 M_{Z_{BL}}^4 (\Gamma_H^2 M_H^2 + (M_H^2 - s)^2)}, \tag{49}$$

$$\begin{aligned}
A_7 = & \left[64 g_{\text{BL}}^4 \sin^2 \theta \cos^2 \theta M_{N_1}^2 (s - 4M_{N_1}^2) (s^2 - 4sM_{Z_{\text{BL}}}^2 + 12M_{Z_{\text{BL}}}^4) \times \right. \\
& \left. (\Gamma_h M_h \Gamma_H M_H + (s - M_h^2)(s - M_H^2)) \right] \times \\
& \frac{1}{9M_{Z_{\text{BL}}}^4 (\Gamma_h^2 M_h^2 + (M_h^2 - s)^2) (\Gamma_H^2 M_H^2 + (M_H^2 - s)^2)}, \tag{50}
\end{aligned}$$

$$\sigma_{Z_{\text{BL}}, Z_{\text{BL}}} = \frac{1}{32\pi s} \frac{\sqrt{1 - \frac{4M_{N_1}^2}{s}}}{\sqrt{1 - \frac{4M_{Z_{\text{BL}}}^2}{s}}} \sum_{i=1}^7 A_i \tag{51}$$

$\mathbf{N}_x \bar{\mathbf{N}}_x \rightarrow \mathbf{N}_1 \bar{\mathbf{N}}_1$ (where N_x s are the other two sterile neutrinos with $x = 2, 3$)

In this annihilation process we have considered the only Z_{BL} mediated s -channel diagram as it contributes dominantly over the other possible diagrams.

$$\begin{aligned}
g_{N_x N_x Z_{\text{BL}}} &= -g_{\text{BL}}(\cos \alpha_x^2 - \sin \alpha_x^2), \\
g_{N_1 N_1 Z_{\text{BL}}} &= -g_{\text{BL}}(\cos \alpha^2 - \sin \alpha^2), \\
\sigma_{N_x N_x} &= \frac{(g_{N_x N_x Z_{\text{BL}}} \times g_{N_1 N_1 Z_{\text{BL}}})^2}{256 \pi s \left[(s - M_{Z_{\text{BL}}}^2)^2 + (\Gamma_{Z_{\text{BL}}} M_{Z_{\text{BL}}})^2 \right]} \frac{\sqrt{s - 4M_{N_1}^2}}{\sqrt{s - 4M_{N_x}^2}} \times \\
& \left[\frac{32 (4M_{N_1}^2 (M_{N_x}^2 (-6sM_{Z_{\text{BL}}}^2 + 7M_{Z_{\text{BL}}}^4 + 3s^2) - sM_{Z_{\text{BL}}}^4) + sM_{Z_{\text{BL}}}^4 (s - 4M_{N_x}^2))}{3M_{Z_{\text{BL}}}^4} \right]. \tag{52}
\end{aligned}$$

Here, α_x is the active-sterile neutrino mixing angle of ν_x with N_x with $x = 1, 2, 3$ and α_1 has been denoted simply by α .

A.3 Total decay widths of Z_{BL} , H and h

The total decay width of different particles used in the expressions for the annihilation cross section are given below :

Total Decay width of Z_{BL}

$$\begin{aligned}
\Gamma(Z_{\text{BL}} \rightarrow f \bar{f}) &= \frac{M_{Z_{\text{BL}}}}{12 \pi} n_c (q_f g_{\text{BL}})^2 \left(1 + \frac{2 M_f^2}{M_{Z_{\text{BL}}}^2}\right) \sqrt{1 - \frac{4 M_f^2}{M_{Z_{\text{BL}}}^2}}, \\
\Gamma(Z_{\text{BL}} \rightarrow \nu_x \bar{\nu}_x) &= \frac{M_{Z_{\text{BL}}}}{24 \pi} ((\cos^2 \alpha_x - \sin^2 \alpha_x)^2 g_{\text{BL}}^2) \left(1 - \frac{4 M_{\nu_x}^2}{M_{Z_{\text{BL}}}^2}\right)^{3/2}, \\
\Gamma(Z_{\text{BL}} \rightarrow N_x \bar{N}_x) &= \frac{M_{Z_{\text{BL}}}}{24 \pi} ((\sin^2 \alpha_x - \cos^2 \alpha_x)^2 g_{\text{BL}}^2) \left(1 - \frac{4 M_{N_x}^2}{M_{Z_{\text{BL}}}^2}\right)^{3/2}.
\end{aligned} \tag{53}$$

$$\Gamma_{Z_{\text{BL}}} = \sum_f \Gamma(Z_{\text{BL}} \rightarrow f \bar{f}) + \sum_{x=1}^3 \left(\Gamma(Z_{\text{BL}} \rightarrow \nu_x \bar{\nu}_x) + \Gamma(Z_{\text{BL}} \rightarrow N_x \bar{N}_x) \right). \tag{54}$$

Total Decay width of H

$$\begin{aligned}
\Gamma(H \rightarrow V V) &= \frac{G_F M_H^3 \sin^2 \theta \delta V}{16 \sqrt{2} \pi} \sqrt{1 - \frac{4 M_V^2}{M_H^2}} \left(1 - \frac{4 M_V^2}{M_H^2} + \frac{12 M_V^4}{M_H^4}\right), \\
\Gamma(H \rightarrow Z_{\text{BL}} Z_{\text{BL}}) &= \frac{g_{\text{BL}}^2 M_H^3 \cos^2 \theta}{8 \pi M_{Z_{\text{BL}}}^2} \sqrt{1 - \frac{4 M_{Z_{\text{BL}}}^2}{M_H^2}} \left(1 - \frac{4 M_{Z_{\text{BL}}}^2}{M_H^2} + \frac{12 M_{Z_{\text{BL}}}^4}{M_H^4}\right), \\
\Gamma(H \rightarrow f \bar{f}) &= \frac{n_c M_H}{8 \pi} \left(\frac{M_f \sin \theta}{v}\right)^2 \left(1 - \frac{4 M_f^2}{M_H^2}\right)^{3/2}, \\
\Gamma(H \rightarrow h h) &= \frac{g_{hhH}^2}{32 \pi M_H} \sqrt{1 - \frac{4 M_h^2}{M_H^2}}, \\
\Gamma(H \rightarrow N_x \bar{N}_x) &= \frac{g_{HN_x N_x}^2 M_H}{16 \pi} \left(1 - \frac{4 M_{N_x}^2}{M_H^2}\right)^{3/2}, \\
\Gamma(H \rightarrow \nu_x \bar{\nu}_x) &= \frac{g_{H\nu_x \nu_x}^2 M_H}{16 \pi} \left(1 - \frac{4 M_{\nu_x}^2}{M_H^2}\right)^{3/2},
\end{aligned} \tag{55}$$

$$\begin{aligned}
\Gamma_H &= \sum_f \Gamma(H \rightarrow f \bar{f}) + \sum_{x=1}^3 \left(\Gamma(H \rightarrow \nu_x \bar{\nu}_x) + \Gamma(H \rightarrow N_x \bar{N}_x) \right) \\
&\quad + \sum_{V=W, Z} \Gamma(H \rightarrow V V) + \Gamma(H \rightarrow Z_{\text{BL}} Z_{\text{BL}}),
\end{aligned} \tag{57}$$

where, $\delta V = 2$ for W boson and 1 for Z boson and

$$g_{HN_x N_x} = 2 \cos \alpha_x \left(\sin \theta \sin \alpha_x \frac{\sqrt{M_{N_x} m_{\nu_x}}}{v} - \cos \theta \cos \alpha_x \frac{g_{\text{BL}} M_{N_x}}{M_{Z_{\text{BL}}}} \right),$$

$$g_{H\nu_x \nu_x} = 2 \sin \alpha_x \left(\sin \theta \cos \alpha_x \frac{\sqrt{M_{N_x} m_{\nu_x}}}{v} + \cos \theta \sin \alpha_x \frac{g_{\text{BL}} M_{N_x}}{M_{Z_{\text{BL}}}} \right).$$

Total Decay width of h

$$\begin{aligned} \Gamma(h \rightarrow Z_{\text{BL}} Z_{\text{BL}}) &= \frac{g_{\text{BL}}^2 M_h^3 \sin^2 \theta}{8 \pi M_{Z_{\text{BL}}}^2} \sqrt{1 - \frac{4 M_{Z_{\text{BL}}}^2}{M_h^2}} \left(1 - \frac{4 M_{Z_{\text{BL}}}^2}{M_h^2} + \frac{12 M_{Z_{\text{BL}}}^4}{M_h^4} \right), \\ \Gamma(h \rightarrow H H) &= \frac{g_{HHh}^2}{32 \pi M_h} \sqrt{1 - \frac{4 M_H^2}{M_h^2}}, \\ \Gamma(h \rightarrow N_x \bar{N}_x) &= \frac{g_{hN_x N_x}^2 M_h}{16 \pi} \left(1 - \frac{4 M_{N_x}^2}{M_h^2} \right)^{3/2}, \\ \Gamma(h \rightarrow \nu_x \bar{\nu}_x) &= \frac{g_{h\nu_x \nu_x}^2 M_h}{16 \pi} \left(1 - \frac{4 M_{\nu_x}^2}{M_h^2} \right)^{3/2}, \\ \Gamma_h &= \cos^2 \theta \Gamma_h^{\text{SM}} + \Gamma(h \rightarrow Z_{\text{BL}} Z_{\text{BL}}) + \Gamma(h \rightarrow H H) \\ &\quad + \sum_{x=1}^3 \left(\Gamma(h \rightarrow \nu_x \bar{\nu}_x) + \Gamma(h \rightarrow N_x \bar{N}_x) \right), \end{aligned} \tag{58}$$

where $\Gamma_h^{\text{SM}} = 4.14 \times 10^{-3}$ MeV [83] is the decay width of SM Higgs boson with mass 125.5 GeV and

$$g_{hN_x N_x} = 2 \cos \alpha_x \left(\cos \theta \sin \alpha_x \frac{\sqrt{M_{N_x} m_{\nu_x}}}{v} + \sin \theta \cos \alpha_x \frac{g_{\text{BL}} M_{N_x}}{M_{Z_{\text{BL}}}} \right),$$

$$g_{h\nu_x \nu_x} = 2 \sin \alpha_x \left(\cos \theta \cos \alpha_x \frac{\sqrt{M_{N_x} m_{\nu_x}}}{v} - \sin \theta \sin \alpha_x \frac{g_{\text{BL}} M_{N_x}}{M_{Z_{\text{BL}}}} \right).$$

A.4 Decay width of $N_1 \rightarrow e^\pm \nu_i$ ($i = 1$ to 3)

In this section, we have calculated the three body decay width of sterile neutrino dark matter N_1 into e^\pm and ν_i . In this calculation we have considered only W^\pm and Z bosons mediated diagrams as these three diagrams contribute dominantly to this decay process of N_1 . Also in our calculation, for simplicity, we have neglected terms involving neutrino masses as these

are extremely tiny compared to the masses of other particles. Further, we have neglected the intergenerational mixing between active and sterile neutrinos. We have define two quantities X and Y in terms of four momentums of ν_i , e^+ and N_1 as

$$X = (P - p_1)^2, \quad (59)$$

$$Y = (P - p_2)^2, \quad (60)$$

where P is four momentum of N_1 while that of ν_i and e^- are p_1 and p_2 respectively. Now,

$$B_1 = \frac{8}{M_Z^4} \left(a_2^2 \left(M_Z^4 (4Y M_e^2 - 2M_e^4 + M_{N_1}^2 (X + 2Y) - X^2 - 2XY - 2Y^2) \right) + a_3^2 \left(M_{N_1}^2 (M_Z^4 \times (X + 2Y) - 2M_e^2 (-2X M_Z^2 + 2M_Z^4 + X^2)) + 2M_e^2 M_{N_1}^4 (X - 2M_Z^2) + M_Z^4 (-(-4M_e^2 \times (X + Y) + 2M_e^4 + X^2 + 2XY + 2Y^2)) \right) \right), \quad (61)$$

$$B_2 = -\frac{16}{M_W^4} \left(M_e^4 (-M_{N_1}^2 (8M_W^2 + 7(X + Y)) + 5M_{N_1}^4 + 4M_W^2 (M_W^2 + X) + (X + Y)^2) + M_e^2 (M_{N_1}^2 (4M_W^2 (M_W^2 + Y) + (X + Y)^2) - M_{N_1}^4 (X + Y) - 8Y M_W^4) - 2M_e^6 (-3M_{N_1}^2 + X + Y) + M_e^8 + 4Y M_W^4 (Y - M_{N_1}^2) \right), \quad (62)$$

$$B_3 = -\frac{16}{M_W^4} \left(M_e^4 (Y M_{N_1}^2 + M_{N_1}^4 + 4M_W^2 (M_W^2 + X) + Y^2) + M_e^2 (M_{N_1}^2 (-4M_W^2 (X + Y) + 4M_W^4 + Y^2) - M_{N_1}^4 (Y - 4M_W^2) - 8M_W^4 (X + Y)) - 2M_e^6 (M_{N_1}^2 + Y) + M_e^8 + 4M_W^4 (X + Y) (-M_{N_1}^2 + X + Y) \right), \quad (63)$$

$$B_4 = -\frac{8}{M_W^2 M_Z^2} \left(a_2 M_Z^2 \left(M_e^4 (M_{N_1}^2 + 2M_W^2 - X - 2Y) + M_e^2 (-M_{N_1}^2 (3X + 2Y) + 2M_{N_1}^4 + 2M_W^2 \times (X - 2Y) + (X + Y)^2) + M_e^6 + 2Y M_W^2 (Y - M_{N_1}^2) \right) + a_3 \left(M_{N_1}^2 (M_Z^2 (-M_e^2 (4M_W^2 + 3X + 4Y) + 5M_e^4 + 2Y M_W^2) + X M_e^2 (-2M_e^2 + 2M_W^2 + X + Y)) + M_e^2 M_{N_1}^4 (M_e^2 - 2M_W^2 + 2M_Z^2 - X) + M_Z^2 (-2M_W^2 (-M_e^2 (X + 2Y) + M_e^4 + Y^2) - M_e^4 (3X + 2Y) + M_e^2 (X + Y)^2 + M_e^6) \right) \right), \quad (64)$$

$$\begin{aligned}
B_5 = & -\frac{8}{M_W^2 M_Z^2} \left(a_2 M_Z^2 \left(M_e^2 (-X M_{N_1}^2 + M_{N_1}^4 - 2M_W^2(X + 2Y) + Y^2) + M_e^4 (-M_{N_1}^2 + 2M_W^2 + X \right. \right. \\
& \left. \left. - 2Y) + M_e^6 + 2M_W^2(X + Y) (-M_{N_1}^2 + X + Y) \right) + a_3 \left(M_e^2 (M_{N_1}^2 (M_Z^2 (-4M_W^2 + X + 2Y) \right. \right. \\
& \left. \left. + 2X M_W^2 - XY) + M_{N_1}^4 (- (2M_W^2 + M_Z^2)) + M_Z^2 (M_W^2(6X + 4Y) + Y^2)) + M_e^4 (M_{N_1}^4 - M_Z^2 \times \right. \right. \\
& \left. \left. (M_{N_1}^2 + 2M_W^2 + X + 2Y)) + M_e^6 M_Z^2 - 2M_W^2 M_Z^2(X + Y) (-M_{N_1}^2 + X + Y) \right) \right) ,
\end{aligned} \tag{65}$$

Also,

$$\begin{aligned}
f_1 &= \left(\frac{e \sin 2\alpha}{2 \sin 2\theta_W} \right)^2, \\
f_2 &= \left(\frac{e^2 \sin 2\alpha}{16 \sin^2 \theta_W} \right)^2, \\
f_3 &= -\frac{e^3 \sin^2 2\alpha}{32 \sin^2 \theta_W \sin 2\theta_W},
\end{aligned} \tag{66}$$

and

$$\begin{aligned}
D_1 &= (X - M_Z^2)^2 + (\Gamma_Z M_Z)^2, \\
D_2 &= (M_{N_1}^2 + M_{\nu_1}^2 + 2M_e^2 - X - Y - M_W^2)^2 + (\Gamma_W M_W)^2, \\
D_3 &= (Y - M_W^2)^2 + (\Gamma_W M_W)^2, \\
D_4 &= D_1 D_2, \\
D_5 &= D_1 D_3,
\end{aligned} \tag{67}$$

with Γ_W and Γ_Z are the total decay widths of W^\pm and Z bosons respectively.

Therefore,

$$\begin{aligned}
|M_1^2| &= \frac{1}{2} \frac{B_1 f_1}{D_1} \times \left(\sum_{\alpha=1}^3 U_{e\alpha}^2 \right), \\
|M_2^2| &= \frac{1}{2} \frac{B_2 f_2}{D_2} \times \left(\sum_{\alpha=1}^3 U_{e\alpha}^4 \right), \\
|M_3^2| &= \frac{1}{2} \frac{B_3 f_2}{D_3} \times \left(\sum_{\alpha=1}^3 U_{e\alpha}^4 \right), \\
|M_4^2| &= \frac{B_4 f_3 [(M_{N_1}^2 + M_{\nu_1}^2 + 2M_e^2 - X - Y - M_W^2)(X - M_Z^2) + \Gamma_W \Gamma_Z M_W M_Z]}{D_4} \times \left(\sum_{\alpha=1}^3 U_{e\alpha}^3 \right), \\
|M_5^2| &= \frac{B_5 f_3 [(Y - M_W^2)(X - M_Z^2) + \Gamma_W \Gamma_Z M_W M_Z]}{D_5} \times \left(\sum_{\alpha=1}^3 U_{e\alpha}^3 \right),
\end{aligned} \tag{68}$$

where $U_{e\alpha}$ s are the elements of PMNS matrix of neutrino mixing and in terms of neutrino mixing angles these are defined as (assuming Dirac CP phase $\delta = 0$)

$$U_{e1} = \cos \theta_{12} \cos \theta_{13}, \quad U_{e2} = \sin \theta_{12} \cos \theta_{13}, \quad U_{e3} = \sin \theta_{13}. \tag{69}$$

Finally, the expression of Matrix amplitude square for the process $N_1 \rightarrow e^\pm \nu_i$ is given by,

$$|M^2| = \sum_1^5 |M_i^2|. \tag{70}$$

The corresponding decay width in terms of $|M^2|$ is given by,

$$\Gamma_{N_1 \rightarrow e^\pm \nu_i} = \frac{1}{2\pi^3} \frac{1}{32 M_{N_1}^3} \int_{Y_{min}}^{Y_{max}} \int_{X_{min}}^{X_{max}} |M^2| dX dY. \tag{71}$$

The upper and lower limits of the quantities X and Y are given below

$$\begin{aligned}
X_{min} &= (x+y)^2 - \left(\sqrt{x^2 - M_e^2} - \sqrt{y^2 - M_e^2} \right)^2, \\
X_{max} &= (x+y)^2 - \left(\sqrt{x^2 - M_e^2} + \sqrt{y^2 - M_e^2} \right)^2,
\end{aligned} \tag{72}$$

with

$$\begin{aligned}
x &= \frac{Y + M_e^2}{2\sqrt{Y}}, \\
y &= \frac{M_{N_1}^2 - Y - M_e^2}{2\sqrt{Y}},
\end{aligned} \tag{73}$$

and

$$\begin{aligned} Y_{min} &= M_e^2, \\ Y_{max} &= (M_{N_1} - M_e)^2. \end{aligned} \tag{74}$$

References

- [1] G. Hinshaw *et al.* [WMAP Collaboration], “*Nine-Year Wilkinson Microwave Anisotropy Probe (WMAP) Observations: Cosmological Parameter Results*”, *Astrophys. J. Suppl.* **208**, 19 (2013) [arXiv:1212.5226 [astro-ph.CO]].
- [2] P. A. R. Ade *et al.* [Planck Collaboration], “*Planck 2015 results. XIII. Cosmological parameters*”, arXiv:1502.01589 [astro-ph.CO].
- [3] Y. Sofue and V. Rubin, “*Rotation curves of spiral galaxies*”, *Ann. Rev. Astron. Astrophys.* **39**, 137 (2001) [astro-ph/0010594].
- [4] M. Bartelmann and P. Schneider, “*Weak gravitational lensing*”, *Phys. Rept.* **340**, 291 (2001) [astro-ph/9912508].
- [5] D. Clowe, A. Gonzalez and M. Markevitch, “*Weak lensing mass reconstruction of the interacting cluster 1E0657-558: Direct evidence for the existence of dark matter*”, *Astrophys. J.* **604**, 596 (2004) [astro-ph/0312273].
- [6] G. Jungman, M. Kamionkowski and K. Griest, “*Supersymmetric dark matter*”, *Phys. Rept.* **267**, 195 (1996) [hep-ph/9506380].
- [7] D. S. Akerib *et al.* [LUX Collaboration], “*Improved Limits on Scattering of Weakly Interacting Massive Particles from Reanalysis of 2013 LUX Data*”, *Phys. Rev. Lett.* **116**, no. 16, 161301 (2016) [arXiv:1512.03506 [astro-ph.CO]].
- [8] E. Aprile *et al.* [XENON100 Collaboration], “*Dark Matter Results from 225 Live Days of XENON100 Data*”, *Phys. Rev. Lett.* **109**, 181301 (2012) [arXiv:1207.5988 [astro-ph.CO]].
- [9] E. Aprile *et al.* [XENON Collaboration], “*Physics reach of the XENON1T dark matter experiment*”, *JCAP* **1604**, no. 04, 027 (2016) [arXiv:1512.07501 [physics.ins-det]].
- [10] D. S. Akerib *et al.* [LZ Collaboration], “*LUX-ZEPLIN (LZ) Conceptual Design Report*”, arXiv:1509.02910 [physics.ins-det].

- [11] C. E. Aalseth *et al.*, “*The DarkSide Multiton Detector for the Direct Dark Matter Search*”, Adv. High Energy Phys. **2015**, 541362 (2015).
- [12] A. Drukier and L. Stodolsky, “*Principles and Applications of a Neutral Current Detector for Neutrino Physics and Astronomy*”, Phys. Rev. D **30**, 2295 (1984).
- [13] P. Cushman *et al.*, “*Working Group Report: WIMP Dark Matter Direct Detection*”, arXiv:1310.8327 [hep-ex].
- [14] W. C. Haxton, R. G. Hamish Robertson and A. M. Serenelli, “*Solar Neutrinos: Status and Prospects*”, Ann. Rev. Astron. Astrophys. **51**, 21 (2013) [arXiv:1208.5723 [astro-ph.SR]].
- [15] F. Mayet *et al.*, “*A review of the discovery reach of directional Dark Matter detection*”, Phys. Rept. **627**, 1 (2016) [arXiv:1602.03781 [astro-ph.CO]].
- [16] L. Covi, J. E. Kim and L. Roszkowski, “*Axinos as cold dark matter*”, Phys. Rev. Lett. **82**, 4180 (1999) [hep-ph/9905212].
- [17] L. Covi, H. B. Kim, J. E. Kim and L. Roszkowski, “*Axinos as dark matter*”, JHEP **0105**, 033 (2001) [hep-ph/0101009].
- [18] K. Y. Choi, J. E. Kim and L. Roszkowski, “*Review of axino dark matter*”, J. Korean Phys. Soc. **63**, 1685 (2013) [arXiv:1307.3330 [astro-ph.CO]].
- [19] R. Kallosh, L. Kofman, A. D. Linde and A. Van Proeyen, “*Gravitino production after inflation*”, Phys. Rev. D **61**, 103503 (2000) [hep-th/9907124].
- [20] G. F. Giudice, A. Riotto and I. Tkachev, “*Thermal and nonthermal production of gravitinos in the early universe*”, JHEP **9911**, 036 (1999) [hep-ph/9911302].
- [21] E. W. Kolb, D. J. H. Chung and A. Riotto, “*WIMPzillas!*”, In *Heidelberg 1998, Dark matter in astrophysics and particle physics 1998* 592-614 [hep-ph/9810361].
- [22] H. Baer, K. Y. Choi, J. E. Kim and L. Roszkowski, “*Dark matter production in the early Universe: beyond the thermal WIMP paradigm*”, Phys. Rept. **555**, 1 (2015) [arXiv:1407.0017 [hep-ph]].
- [23] L. J. Hall, K. Jedamzik, J. March-Russell and S. M. West, “*Freeze-In Production of FIMP Dark Matter*”, JHEP **1003**, 080 (2010) [arXiv:0911.1120 [hep-ph]].
- [24] B. Shakya, “*Sterile Neutrino Dark Matter from Freeze-In*”, Mod. Phys. Lett. A **31**, no. 06, 1630005 (2016) [arXiv:1512.02751 [hep-ph]].

- [25] J. McDonald, “*Thermally generated gauge singlet scalars as selfinteracting dark matter*”, Phys. Rev. Lett. **88**, 091304 (2002) [hep-ph/0106249].
- [26] C. E. Yaguna, “*The Singlet Scalar as FIMP Dark Matter*”, JHEP **1108**, 060 (2011) [arXiv:1105.1654 [hep-ph]].
- [27] A. Biswas, D. Majumdar and P. Roy, “*Nonthermal two component dark matter model for Fermi-LAT γ -ray excess and 3.55 keV X-ray line*”, JHEP **1504**, 065 (2015) [arXiv:1501.02666 [hep-ph]].
- [28] F. Elahi, C. Kolda and J. Unwin, “*UltraViolet Freeze-in*”, JHEP **1503**, 048 (2015) [arXiv:1410.6157 [hep-ph]].
- [29] S. B. Roland, B. Shakya and J. D. Wells, “*Neutrino Masses and Sterile Neutrino Dark Matter from the PeV Scale*”, Phys. Rev. D **92**, no. 11, 113009 (2015) [arXiv:1412.4791 [hep-ph]].
- [30] P. S. Bhupal Dev, A. Mazumdar and S. Qutub, “*Constraining Non-thermal and Thermal properties of Dark Matter*”, Front. in Phys. **2**, 26 (2014) [arXiv:1311.5297 [hep-ph]].
- [31] M. Endo and F. Takahashi, “*Non-thermal Production of Dark Matter from Late-Decaying Scalar Field at Intermediate Scale*”, Phys. Rev. D **74**, 063502 (2006) [hep-ph/0606075].
- [32] M. Shaposhnikov and I. Tkachev, “*The nuMSM, inflation, and dark matter*”, Phys. Lett. B **639**, 414 (2006) [hep-ph/0604236].
- [33] N. Okada and O. Seto, “*Higgs portal dark matter in the minimal gauged $U(1)_{B-L}$ model*”, Phys. Rev. D **82**, 023507 (2010) [arXiv:1002.2525 [hep-ph]].
- [34] T. Basak and T. Mondal, “*Constraining Minimal $U(1)_{B-L}$ model from Dark Matter Observations*”, Phys. Rev. D **89**, 063527 (2014) [arXiv:1308.0023 [hep-ph]].
- [35] W. Rodejohann and C. E. Yaguna, “*Scalar dark matter in the B-L model*”, JCAP **1512**, no. 12, 032 (2015) [arXiv:1509.04036 [hep-ph]].
- [36] A. Biswas, S. Choubey and S. Khan, “*Galactic Gamma Ray Excess and Dark Matter Phenomenology in a $U(1)_{B-L}$ Model*”, arXiv:1604.06566 [hep-ph].
- [37] S. Dodelson and L. M. Widrow, “*Sterile-neutrinos as dark matter*”, Phys. Rev. Lett. **72**, 17 (1994) [hep-ph/9303287].

- [38] R. Essig *et al.*, “*Constraining Light Dark Matter with Diffuse X-Ray and Gamma-Ray Observations*”, JHEP **1311**, 193 (2013) [arXiv:1309.4091 [hep-ph]].
- [39] X. D. Shi and G. M. Fuller, “*A New dark matter candidate: Nonthermal sterile neutrinos*”, Phys. Rev. Lett. **82**, 2832 (1999) [astro-ph/9810076].
- [40] S. B. Roland, B. Shakya and J. D. Wells, “*PeV neutrinos and a 3.5 keV x-ray line from a PeV-scale supersymmetric neutrino sector*”, Phys. Rev. D **92**, no. 9, 095018 (2015) [arXiv:1506.08195 [hep-ph]].
- [41] K. Kadota, “*Sterile neutrino dark matter in warped extra dimensions*”, Phys. Rev. D **77**, 063509 (2008) [arXiv:0711.1570 [hep-ph]].
- [42] M. Frigerio and C. E. Yaguna, “*Sterile Neutrino Dark Matter and Low Scale Leptogenesis from a Charged Scalar*”, Eur. Phys. J. C **75**, no. 1, 31 (2015) [arXiv:1409.0659 [hep-ph]].
- [43] A. Merle, V. Niro and D. Schmidt, “*New Production Mechanism for keV Sterile Neutrino Dark Matter by Decays of Frozen-In Scalars*”, JCAP **1403**, 028 (2014) [arXiv:1306.3996 [hep-ph]].
- [44] A. Merle and M. Totzauer, “*keV Sterile Neutrino Dark Matter from Singlet Scalar Decays: Basic Concepts and Subtle Features*”, JCAP **1506**, 011 (2015) [arXiv:1502.01011 [hep-ph]].
- [45] B. Shuve and I. Yavin, “*Dark matter progenitor: Light vector boson decay into sterile neutrinos*”, Phys. Rev. D **89**, no. 11, 113004 (2014) [arXiv:1403.2727 [hep-ph]].
- [46] K. Kaneta, Z. Kang and H. S. Lee, “*Right-handed neutrino dark matter under the B-L gauge interaction*”, arXiv:1606.09317 [hep-ph].
- [47] G. Gelmini, S. Palomares-Ruiz and S. Pascoli, “*Low reheating temperature and the visible sterile neutrino*”, Phys. Rev. Lett. **93**, 081302 (2004) [astro-ph/0403323].
- [48] G. Gelmini, E. Osoba, S. Palomares-Ruiz and S. Pascoli, “*MeV sterile neutrinos in low reheating temperature cosmological scenarios*”, JCAP **0810**, 029 (2008) [arXiv:0803.2735 [astro-ph]].
- [49] S. Khalil and O. Seto, “*Sterile neutrino dark matter in B-L extension of the standard model and galactic 511-keV line*”, JCAP **0810**, 024 (2008) [arXiv:0804.0336 [hep-ph]].
- [50] J. Knodlseder *et al.*, “*Early SPI / INTEGRAL constraints on the morphology of the 511 keV line emission in the 4th galactic quadrant*”, Astron. Astrophys. **411**, L457 (2003) [astro-ph/0309442].

- [51] G. Aad *et al.* [ATLAS Collaboration], “*Observation of a new particle in the search for the Standard Model Higgs boson with the ATLAS detector at the LHC*”, Phys. Lett. B **716**, 1 (2012) [arXiv:1207.7214 [hep-ex]].
- [52] S. Chatrchyan *et al.* [CMS Collaboration], “*Observation of a new boson at a mass of 125 GeV with the CMS experiment at the LHC*”, Phys. Lett. B **716**, 30 (2012) [arXiv:1207.7235 [hep-ex]].
- [53] T. Mondal and T. Basak, “*Class of Higgs-portal Dark Matter models in the light of gamma-ray excess from Galactic center*”, Phys. Lett. B **744**, 208 (2015) [arXiv:1405.4877 [hep-ph]].
- [54] A. Hook, E. Izaguirre and J. G. Wacker, “*Model Independent Bounds on Kinetic Mixing*”, Adv. High Energy Phys. **2011**, 859762 (2011) [arXiv:1006.0973 [hep-ph]].
- [55] L. Basso, A. Belyaev, S. Moretti and C. H. Shepherd-Themistocleous, “*Phenomenology of the minimal B-L extension of the Standard model: Z' and neutrinos*”, Phys. Rev. D **80**, 055030 (2009) [arXiv:0812.4313 [hep-ph]].
- [56] M. Carena, A. Daleo, B. A. Dobrescu and T. M. P. Tait, “*Z' gauge bosons at the Tevatron*”, Phys. Rev. D **70**, 093009 (2004) [hep-ph/0408098].
- [57] G. Cacciapaglia, C. Csaki, G. Marandella and A. Strumia, “*The Minimal Set of Electroweak Precision Parameters*”, Phys. Rev. D **74**, 033011 (2006) [hep-ph/0604111].
- [58] G. Aad *et al.* [ATLAS Collaboration], “*Search for high-mass dilepton resonances in pp collisions at $\sqrt{s} = 8$ TeV with the ATLAS detector*”, Phys. Rev. D **90**, no. 5, 052005 (2014) [arXiv:1405.4123 [hep-ex]].
- [59] P. Gondolo and G. Gelmini, “*Cosmic abundances of stable particles: Improved analysis*”, Nucl. Phys. B **360**, 145 (1991).
- [60] G. Arcadi and L. Covi, “*Minimal Decaying Dark Matter and the LHC*”, JCAP **1308**, 005 (2013) [arXiv:1305.6587 [hep-ph]].
- [61] K. A. Olive *et al.* [Particle Data Group Collaboration], “*Review of Particle Physics*”, Chin. Phys. C **38**, 090001 (2014).
- [62] P. Bechtle, S. Heinemeyer, O. Stål, T. Stefaniak and G. Weiglein, “*Probing the Standard Model with Higgs signal rates from the Tevatron, the LHC and a future ILC*”, JHEP **1411**, 039 (2014) [arXiv:1403.1582 [hep-ph]].

- [63] A. Boyarsky, J. Lesgourgues, O. Ruchayskiy and M. Viel, “*Lyman-alpha constraints on warm and on warm-plus-cold dark matter models*”, JCAP **0905**, 012 (2009) [arXiv:0812.0010 [astro-ph]].
- [64] U. Seljak, A. Makarov, P. McDonald and H. Trac, “*Can sterile neutrinos be the dark matter?*”, Phys. Rev. Lett. **97**, 191303 (2006) [astro-ph/0602430].
- [65] A. Boyarsky, J. Lesgourgues, O. Ruchayskiy and M. Viel, “*Realistic sterile neutrino dark matter with keV mass does not contradict cosmological bounds*”, Phys. Rev. Lett. **102**, 201304 (2009) [arXiv:0812.3256 [hep-ph]].
- [66] K. Abazajian, G. M. Fuller and M. Patel, “*Sterile neutrino hot, warm, and cold dark matter*”, Phys. Rev. D **64**, 023501 (2001) [astro-ph/0101524].
- [67] K. S. Babu and R. N. Mohapatra, “*7 keV Scalar Dark Matter and the Anomalous Galactic X-ray Spectrum*”, Phys. Rev. D **89**, 115011 (2014) [arXiv:1404.2220 [hep-ph]].
- [68] J. Edsjo and P. Gondolo, “*Neutralino relic density including coannihilations*”, Phys. Rev. D **56**, 1879 (1997) [hep-ph/9704361].
- [69] J. R. Primack, “*Dark matter and structure formation*”, astro-ph/9707285.
- [70] J. Diemand and B. Moore, “*The structure and evolution of cold dark matter halos*”, Adv. Sci. Lett. **4**, 297 (2011) [arXiv:0906.4340 [astro-ph.CO]].
- [71] T. Siegert *et al.*, “*Gamma-ray spectroscopy of Positron Annihilation in the Milky Way*”, Astron. Astrophys. **586**, A84 (2016) [arXiv:1512.00325 [astro-ph.HE]].
- [72] J. Knodlseder *et al.*, “*The All-sky distribution of 511 keV electron-positron annihilation emission*”, Astron. Astrophys. **441**, 513 (2005) [astro-ph/0506026].
- [73] L. Boubekur, S. Dodelson and O. Vives, “*Cold Positrons from Decaying Dark Matter*”, Phys. Rev. D **86**, 103520 (2012) [arXiv:1206.3076 [astro-ph.CO]].
- [74] E. J. Chun and H. B. Kim, “*Axino Light Dark Matter and Neutrino Masses with R-parity Violation*”, JHEP **0610**, 082 (2006) [hep-ph/0607076].
- [75] D. P. Finkbeiner and N. Weiner, “*Exciting Dark Matter and the INTEGRAL/SPI 511 keV signal*”, Phys. Rev. D **76**, 083519 (2007) [astro-ph/0702587].
- [76] D. Hooper *et al.*, “*Possible evidence for MeV dark matter in dwarf spheroidals*”, Phys. Rev. Lett. **93**, 161302 (2004) [astro-ph/0311150].

- [77] N. Prantzos *et al.*, “*The 511 keV emission from positron annihilation in the Galaxy*”, Rev. Mod. Phys. **83**, 1001 (2011) [arXiv:1009.4620 [astro-ph.HE]].
- [78] R. J. Wilkinson, A. C. Vincent, C. Boehm and C. McCabe, “*Ruling out the light WIMP explanation of the galactic 511 keV line*”, arXiv:1602.01114 [astro-ph.CO].
- [79] C. Picciotto and M. Pospelov, “*Unstable relics as a source of galactic positrons*”, Phys. Lett. B **605**, 15 (2005) [hep-ph/0402178].
- [80] Y. Ascasibar, P. Jean, C. Boehm and J. Knoedlseder, “*Constraints on dark matter and the shape of the Milky Way dark halo from the 511-keV line*”, Mon. Not. Roy. Astron. Soc. **368**, 1695 (2006) [astro-ph/0507142].
- [81] C. Boehm, D. Hooper, J. Silk, M. Casse and J. Paul, “*MeV dark matter: Has it been detected?*”, Phys. Rev. Lett. **92**, 101301 (2004) [astro-ph/0309686].
- [82] M. Cirelli *et al.*, “*PPPC 4 DM ID: A Poor Particle Physicist Cookbook for Dark Matter Indirect Detection*”, JCAP **1103**, 051 (2011) Erratum: [JCAP **1210**, E01 (2012)] [arXiv:1012.4515 [hep-ph]].
- [83] A. Denner *et al.*, “*Standard Model Higgs-Boson Branching Ratios with Uncertainties*”, Eur. Phys. J. C **71**, 1753 (2011) [arXiv:1107.5909 [hep-ph]].